# University of Alberta

The Effects of Docosahexaenoic Acid (DHA) Dietary Supplementation in a Mouse Model of Stargardt-like Macular Dystrophy (STGD3)

by

Mandy Hong

A thesis submitted to the Faculty of Graduate Studies and Research
in partial fulfillment of the requirements for the degree of

Master of Science

Centre for Neuroscience


Fall 2013
Edmonton, Alberta

## Abstract

Underlying mechanisms of how docosahexaenoic acid (DHA) might impact the progression of macular degeneration are unknown. We relied on the ELOVL4 mouse model of juvenile macular degeneration, STGD3, to test the hypothesis that antenatal DHA dietary supplementation (2% w/w of total fatty acid) would slow down the progression of retinal degeneration as evidenced by preserved function, anatomy, and DHA levels. DHA+, DHA-, and chow diets commenced antenatally. Retina function was assessed by electroretinogram at 1 and 3 months, while anatomical integrity and fatty acid profiles were assessed with cross-sectional staining and UPLC/MS/MS, respectively, at 3 months. Results showed a negative ELOVL4 genotype effect on rod function, photoreceptor numbers, and DHA/AA levels. Surprisingly, in transgenic retinas DHA supplementation resulted in lower DHA levels compared to non-supplemented. Although beneficial effects of DHA have been reported, antenatal and 3 month postnatal supplementation is not sufficient to elicit these effects in mice with STGD3.

**Acknowledgments**

Much of my growth and understanding in this field of research is due in large part to the support and guidance I received from Dr. Yves Sauvé and for that, I am exceedingly grateful. I wish to also thank my committee members, Dr. Ted Allison and Dr. Cathy Chan, for their intellectual contributions, assistance, and understanding throughout my journey in my graduate studies.

The many hours spent in the laboratory have been made invaluable by my interactions with Sharee Kuny and John Dimopoulos. I am thankful not only for the technical knowledge and critical thinking skills I have gained through them, but for the companionship they offered.

Many thanks to Dr. Miyoung Suh for her advice and assistance in the lipid extraction and analysis portion of this project and to Rachel Bryant for the summer she spent in helping me image and count photoreceptor cells.

Finally, without the unending love and encouragement from my parents, sister, and extended family members I would not have come so far in my academic career.

**Table of Contents**

**List of Tables**



***Supplementary Tables***

**List of Figures**



***Supplementary Figures***

**List of Abbreviations**

A2E- Vitamin A derived pyridinium bisretinoid

AA - arachidonic acid

ABCA4 - ATP-binding cassette, subfamily A, member 4 gene

AC - amacrine cell

ALA - α-linolenic acid

AMD - age-related macular degeneration

ANOVA - analysis of variance

ANSA - analine naphthalene sulfonic acid

AREDS - Age-Related Eye Disease Study

ARVO - Association of Research in Vision and Ophthalmology

CBC - cone-driven bipolar cell

CEP - carboxyethlypyrrole

CFH - complement factor H

cGMP - cyclic guanosine monophosphate

CNG - cyclic nucleotide gated

DAPI - 4'-6-Diamidino-2-phenylindole

DHA - docosahexaenoic acid

DNA - deoxyribonucleic acid

DPA - docosapentaenoic acid

ELOVL4 - gene or protein related to elongation of very long chain fatty acids

EPA - eicopentaenoic acid

ER - endoplasmic reticulum

ERG - electroretinogram

FDA - food and drug administration

GCL - ganglion cell layer

GDP - guanosine diphosphate

GMP - guanosine monophosphate

GTP - guanosine triphosphate

HC - horizontal cell

INL - inner nuclear layer

IPL - inner plexiform layer

IRBP - interphotoreceptor retinoid-binding protein

LA - linoleic acid

LC-PUFA - long chain polyunsaturated fatty acid

mGLUR6 - metabotropic glutamate receptor 6

MS - mass spectrometry

NKCX - sodium potassium calcium exchanger

NPD1 - neuroprotectin D1

OCT - optimal cutting temperature resin

OCT - optical coherence tomography

ONL - outer nuclear layer

OPL - outer plexiform layer

PBS - phosphate buffer saline

PDE - phosphodiesterase

PFA - paraformaldehyde

PIR - photopic intensity response

PVC - polyvinyl chloride

RBC - rod-driven bipolar cell

RPE - retinal pigmented epithelium

SEM - standard error of mean

SIR - scotopic intensity response

STGD3 - Stargardt-like macular dystrophy

TG - transgenic

UPLC ultra performance liquid chromatography

UPR - unfolded protein response

VEGF - vascular endothelial growth factor

VLCPUFA - very long chain polyunsaturated fatty acid

WT - wild-type

w/v - weight over volume

w/w - weight over weight

# Chapter 1. INTRODUCTION

## 1.1) Macular Degeneration

The cause of irreversible blindness in developed countries is mainly attributed to macular degeneration. Despite being a pan-retinal disease, the macula is affected first and is the most vulnerable to damage. The locus of injury results in the loss of sharp, central vision and afflicted individuals are often unable to drive vehicles, enjoy reading, or perform ordinary tasks because they must rely solely on their peripheral vision. The phenotype of the disease depends on multiple interacting factors including age, genetics, lifestyle, and environment.

### *1.1A) Late onset: Age-related Macular Degeneration*

Age-related macular degeneration (AMD) earns its name for its characterization as a progressive, neurodegenerative disease that is primarily predicted by age. The disease predominantly concerns individuals over 55 years of age, but by the age of 75 up to 1 in 4 individuals will be affected (Ambati & Fowler, 2012; Soubrane et al, 2002). To date, over 2 million Canadians are affected and the amount of cases are increasing at a rate of 77, 000 per year (Swaroop et al, 2009; Hooper et al, 2005). Similar to other age-related neurodegenerative diseases, AMD is initially presented with an accumulation of extracellular toxins (Bird, 2010; Ding et al, 2009). Accretion of drusen, a protein and lipid-containing substance, in AMD is analogous to extracellular deposits of Tau, huntingtin, and Lewy body proteins described in Alzheimer's, Huntington's, and Parkinson's disease, respectively (Kaarniranta et al, 2011; Ross & Poirier,

2005). The similarity in disease presentation emphasizes the urgency in discovering the molecular mechanisms unifying the development of these neurodegenerative disorders.

It is understood that the accumulation of toxic debris in AMD is detrimental to vision. Aside from drusen formation between the retinal pigmented epithelium (RPE) and choroid, lipofuscin, a lipid-containing residue, can be discovered within RPE cells. The collective effects of lipofuscin and drusen accumulation can result in disrupted functioning of the RPE and photoreceptor cells and subsequent visual impairment. This early stage of disease is known as dry AMD (Ambati & Fowler, 2012; Swaroop et al, 2009; Figure 1). RPE and photoreceptor atrophy, depicted as depigmented regions in fundus photography are a hallmark of dry AMD and are known as geographic atrophy (Khandhadia et al, 2011). The prognosis of the disease can also be inferred by the appearance of drusens. Soft drusen are more diffuse, ill-defined, and more damaging than hard drusen which are specifically located (Williams et al, 2009). Should the disease progress further, the deteriorating and oxygen deprived retina is infiltrated by leaky blood vessels. Constant aggravation of the RPE from toxic accumulation and high metabolic demands induce complement activation and oxidative stress (Khandhadia et al, 2012; Luthert, 2011). In response, the RPE produces and secretes pro-angiogenic factors (Nussenblatt & Ferris, 2007) which lead to a phenomenon known as choroidal neovascularization. Neovascularization disrupts photon reception of photoreceptors but also causes scarring from leakage of blood and proteins in the extracellular environment. At this stage, patients lose 80-90%

of their vision and are diagnosed with wet AMD (Cheung & Eaton, 2013); Figure 1). If left untreated, this can lead to complete blindness. Though only 10 – 15% of AMD cases are classified in this category (Ambati & Fowler, 2012; Damico et al, 2012), the only treatment for AMD approved by the Food and Drug Administration (FDA) is for wet AMD (Kolb et al, 1995). Currently, physicians focus on the use of anti-VEGF (Lally et al, 2012; Cuilla & Rosenfeld, 2009), an antagonist of pro-angiogenic factor vascular endothelial growth factor (VEGF). The results of these treatments are viewed with positivity; however anti-VEGF injections are invasive and expensive. Other potential targets are to inhibit pro-angiogenic molecules or gene therapy (Wang et al, 2012). Complement factor H (CFH) and other complement and immune related genes are known to be largely involved in AMD development; hence, regulation of these gene expressions could greatly impact disease progression (Damico et al, 2012). The majority of AMD cases, however, are without any form of treatment or preventative therapy. For this reason, extensive research is underway to uncover potential remedies for early, dry AMD and to prevent further progression to the wet form.

1

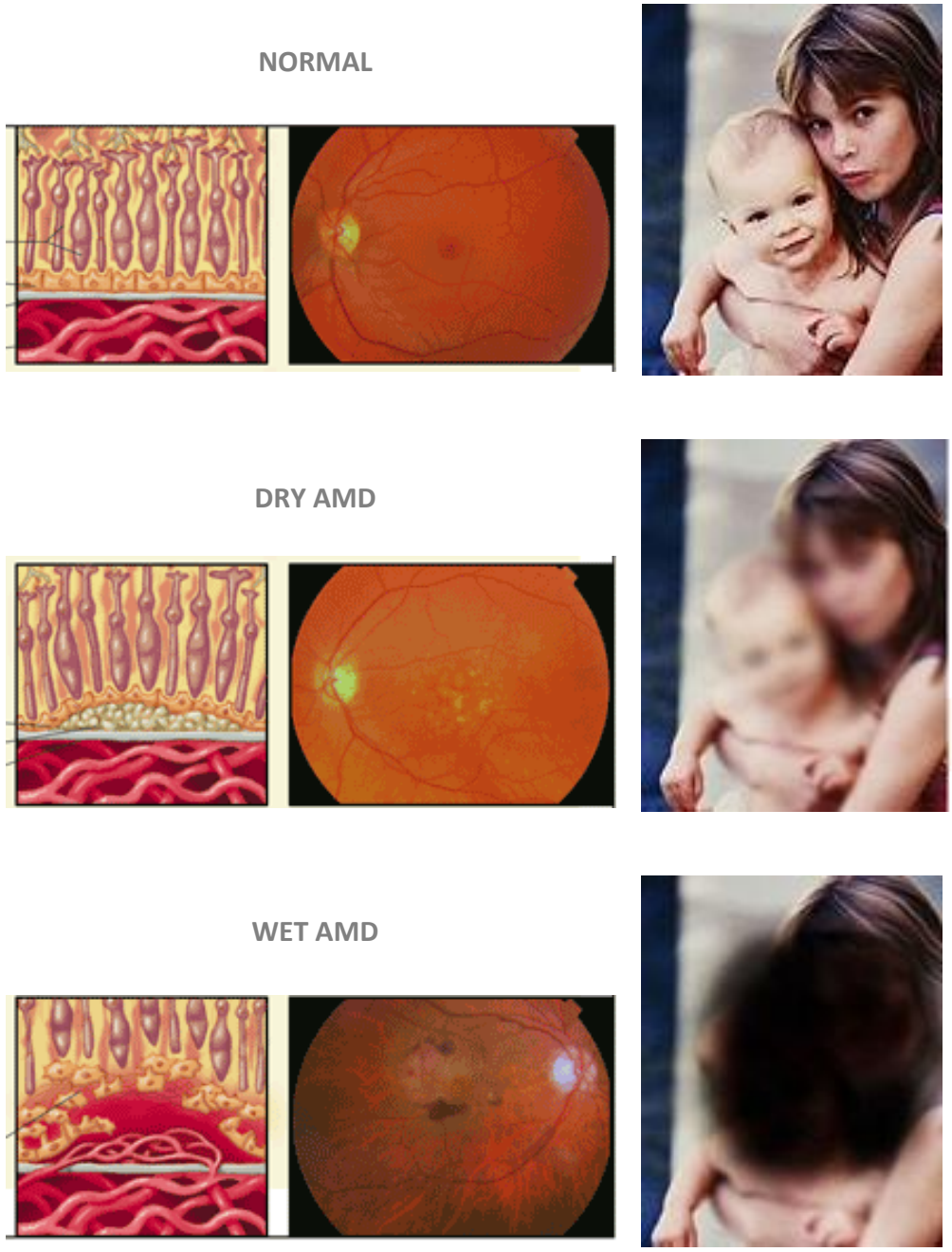


***Figure 1.*** **Pathology of AMD.** Dry AMD: accumulation of extracellular drusen beneath the RPE results in blurred central vision. Wet AMD: infiltration of choroidal vasculature into retinal space causes complete central vision loss. Image derived from healthplexus.net.

### *1.1B) Early Onset: Stargardt-like Macular Dystrophy*

Juvenile macular dystrophy and early, dry AMD share similar clinical profiles. Both forms of macular degeneration demonstrate central retina atrophy, decreased visual acuity, and lipofuscin accumulation (Molday & Zhang, 2010; Rotendtreich et al, 2003; Donoso et al, 2001). What differentiates juvenile macular dystrophy from AMD, and makes it significantly easier to study, are the age of onset and the simple, monogenetic Mendelian pattern of inheritance. Typically, individuals with juvenile macular dystrophies are diagnosed before the age of 20 and have a monogenic predisposition to develop this disease (Molday & Zhang, 2010). Those with an autosomal recessive or dominant gene are identified as having Stargardt or Stargardt-like macular dystrophy, respectively. In the more common recessive form, a mutation in the ATP-binding cassette transporter (subfamily A, member 4), *ABCA4*, gene and consequent production of abnormal ABCA4 proteins results in lipofuscin accumulation (Molday et al 2009). Without the full function of these proteins, which are normally expressed in rod outer segments, the photoreceptors struggle with the removal of N-retinyl-phosophotidylethanolamine (NR-PE).This intracellular debris is further oxidized into *N*-retinylidene-*N*-retinyl-phosphatidyl-ethanolamine (A2PE) in photoreceptors and hydrolyzed into *N*-retinylidene-*N*-retinyl-ethanolamine (A2E), a major constituent of lipofuscin, in the RPE (Molday et al 2009). Thus, RPE and photoreceptor function is compromised and symptoms of macular degeneration arise.

Stargardt-like macular dystrophy, on the other hand, is caused by a mutation in the *ELOVL4* gene. This gene is responsible for encoding an enzyme required for the **el**ongation **o**f **v**ery **l**ong chain fatty acids consisting of 28 carbons or more (Vasireddy et al, 2010). Case studies of multiple families with this disease have assisted researchers in discovering this gene on chromosome 6 (Logan et al, 2012; Zhang et al, 2001). Further genetic analysis identified the mutation in exon 6 of the *ELOVL4* gene. A 5 base-pair deletion, 2 single point mutations, and a frameshift mutation have all been recognized as forms of *ELOVL4* gene mutation (Vasireddy et al, 2010; Figure 2). Regardless, these all result in a premature stop codon and the truncation of the ELOVL4 protein. There are 2 main effects: 1) the loss of the carboxyl terminal containing the endoplasmic reticulum (ER) retention signal and 2) the inability to generate fatty acids with at least 28 carbon chains (Karan et al, 2005). First, loss of the ER retention signal results in the mislocalization of the ELOVL4 protein, saturation of proteosomes, and eventually, initiation of the unfolded protein response (UPR). Failure to resolve the UPR will lead to cellular apoptosis (Karan et al, 2005). In vivo studies have also specified a dominant negative effect of the mutant protein. When expressed together, mutant ELOVL4 protein will sequester the wild-type protein and form aggregates, further overwhelming proteosome capacity (Grayson & Molday, 2005; Vasireddy et al, 2005). The ER, coincidentally, is also where elongation of fatty acids normally occurs. Secondly, very long chain polyunsaturated fatty acids (VLC-PUFAs) are abundant in photoreceptor cells (Agbaga et al, 2010). Disruption in the production of VLC-PUFAs can alter the

lipid integrity of these cells and compromise their function (Agbaga et al, 2008). This mutation, thus, illustrates the importance of fatty acid metabolism in retinal function. The subsequent combined effects of protein mislocalization and reduced VLC-PUFA production result in the clinical symptoms observed in STGD3.

Obtaining a clearer understanding of the precise mechanisms involved in STDG3 may bring light to the development of dry AMD. Current treatments are not yet available for early onset macular degeneration; however dietary supplementation of anti-oxidants and DHA has displayed correlations with improved retinal health (Evans & Lawrenson, 2012; Gehrs et al, 2006).

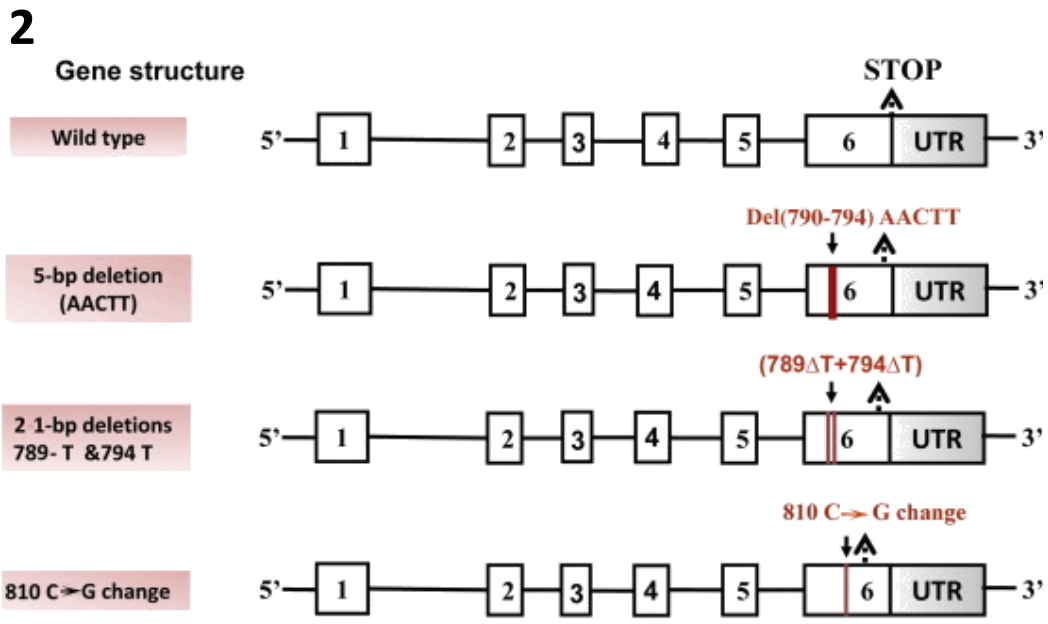


***Figure 2.*** **Mutations in the human *ELOVL4* gene.** All discovered STGD3-causing mutations of the human *ELOVL4* gene occur in exon 6 and results in a premature stop codon. Image from Vasireddy et al, 2010.

### 1.2) Mouse Models of Stargardt-like Macular Dystrophy

Requiring more feasible research tools to advance future therapies for STGD3 and early AMD and also recognizing the similarities between the effects of the *ELOVL4* mutation to the clinical presentation of dry AMD, researchers have generated mouse models of STGD3. For several reasons, animal models are often utilized to study complex disease mechanisms. The mouse in particular is a relatively inexpensive model and upholds a similar genome to humans (90% in likeness; Vasireddy et al, 2010), a fairly short lifespan, and numerous genes and proteins with established antibodies. A chief critique of this animal model, however, is its viability in studying macular degeneration when it, in fact, lacks a macula (Zeiss, 2010). In defense, it is important to recognize macular degeneration as a disease that affects the entire retina (Vasireddy et al, 2010; Marmorstein & Marmorstein, 2007). The mechanisms of the disease, therefore, should not differ greatly from those specific to the macula. Apart from the lack of a macula, the retina structure of mice differs slightly from humans. This can be attributed the fact that mice are nocturnal while humans are diurnal. For this reason, mice retinas are composed of only 2% cone photoreceptors while human retinas contain about 5%. Difference in retina composition can result in differences in retinal disease progression, so it is important to be cautious and aware of the vulnerabilities that are inherent in the mice retina. Acknowledging the advantages and shortcomings of using a mouse model, researchers can effectively use this model to uncover unknown features of STGD3 and possibly early AMD.

Li et al (2007a) and Raz-Prag et al (2006) generated *Elovl4* knock-out mouse models by inserting either a pGneo or LacZ-pGneo cassette into exon 2 of endogenous mice *Elovl4* genes. The deletion in this gene results in the inability of the *Elovl4* allele to express the protein. Using this model, researchers were able to eliminate the possibility that haploinsufficiency is the mechanism by which STDG3 develops. The premise is that to be determined as haploinsufficient, the disease phenotype must be observed if the singular expression of the functional wild-type gene is unable to mask the effects of the mutated gene. This experiment demonstrated that heterozygous knock-out mice were comparable to control mice in regards to fundus appearance, retinal responses, and retinal and RPE thickness. That is, the expression of the wild-type gene alone is sufficient to create normal phenotype. In the same model, homozygous expression of the knock-out genes was lethal, with pups dying within a few hours.

Alternatively, knock-in mouse models were created by introducing the 5 base pair deletion (Vasireddy et al., 2006) into the mouse *Elovl4* homolog via homologous recombination. In this heterozygous model, progressive photoreceptor loss, RPE thickening, lipofuscin accumulation, and altered fatty acid levels were all observed. Interestingly, photoreceptor and bipolar cell activity measured as a- and b-wave amplitudes from electroretinography (ERG), respectively, were significantly enhanced in these animals compared to wild-type (WT) mice at 8 months, but returned to normal responses by 15 months. This model replicated many of the clinical features described in human STGD3 patients and would make an excellent model to study this disease. A setback,

however, is that, similar to the knock-out model, homozygous expression of the knock-in gene results in premature death. These homozygous animals are consistently born with skin abnormalities, appearing dry, wrinkly, and scaly. Acknowledging its vital presence in brain and skin tissue, researchers analyzed fatty acid contents in skin tissue of homozygous mice and found a significant reduction in fatty acids with carbon chains longer than 28 compared to WT animals (Vasireddy et al, 2007; Cameron et al, 2007; McMahon et al, 2007). Conversely, C26 fatty acids were drastically increased. It was inferred from these results that fatty acids of carbon chain lengths of 26 act as substrates for the ELOVL4 enzyme to facilitate elongation of C>28 FA.

Finally, transgenic ELOVL4 mice have also been engineered that have the utility for eye research as well. This model was generated by integrating the human *ELOVL4* gene into the mouse genome under the direction of a photoreceptor specific promoter, IRBP. Using in situ hybridization, Karan et al (2005) were able to confirm that expression of this transgene is uniform throughout the entire retina. The same research group created 3 mouse lines that were differentiated by the level of WT and mutant *ELOVL4* expressed in their genome. TG1 mice expressed the lowest levels of the mutant transgene, while TG2 and TG3 mice expressed progressively higher levels (Karan et al, 2005). Reduced retinal responses, fundus abnormalities, RPE and photoreceptor atrophy, truncated rod outer segments, lipofuscin accumulation, as well as altered neurotrophic and inflammatory gene and protein expression (Kuny et al, 2012; Vasireddy et al, 2010; Vasireddy et al, 2009) were all reported in these animals

and the severity of each phenotype varied directly with the level of transgene expression. Display of the diseased phenotype in the context of joint expression of the WT and mutant genes and their respective gene products verify the dominant negative effect underlying STDG3.

Already, mouse models of STDG3 have contributed to insights in mechanisms related to retinal degeneration. This only serves to emphasize the necessity of pertinent animal models to study disease pathology and explore any potential treatments or therapies.

**1. 3) Docosahexaenoic Acid**

Benefits related to docosahexaenoic acid (DHA) intake on cardiac health (Breslow, 2006), brain development (Morse, 2012), dermatology (Koch et al, 2008), and eye health (Dornstauder et al, 2012; Bazan et al, 2011; Querques et al, 2011; SanGiovanni & Chew, 2005) have been reported repeatedly. Taking this into account, it is promising that DHA could be implemented as a form of disease prevention. To better understand how DHA promotes health benefits, it is important to be familiar with its functional structure and its practical nature. DHA is classified as an omega-3 long chain polyunsaturated fatty acid (LCPUFA). It consists of a 22 carbon chain length, 6 unsaturated bonds, and an initial double bond located 3 carbons from the methyl (or omega) terminal; hence, DHA is also referred to as C22:6n-3 by it chemical name (Figure 3). The body is unable to produce omega-3 and omega-6 fatty acids endogenously, and thus relies on exogenous ingestion of these essential nutrients (Querques et al, 2011). In their

simplest form, omega-3 and 6 fatty acids can be found in flax seeds or canola oil as α-linolenic acid (ALA) or linoleic acid (LA), respectively (SanGiovanni & Chew, 2005). These fatty acids undergo a series of metabolic alterations via elongases and desaturases before arriving as either arachidonic acid (AA) or DHA. Unfortunately, in today's Western diet the intake of omega-3 to omega-6 is grossly imbalanced in favour of omega-6. The consumption of overly processed foods containing corn is what likely contributes to the 10:1 omega-6 to omega-3 ratio observed today (Simopoulos, 1999). The recommended ratio is approximately 1:1 (Querques et al, 2011). An imbalanced diet can be detrimental on cardiac and general health for it has been established that AA and other omega 6 fatty acids promote inflammatory responses, affecting platelet activity, smooth muscle contraction, and thrombosis (Johnson & Fritsche, 2012; Querques et al, 2011).

DHA plays a vital role in visual function as well. It is the most abundant fatty acid, accounting for 50% of total FA, in the photoreceptor outer segments (Tuo et al, 2009; Rotstein et al, 2003). The lipophilic nature of DHA allows it to maintain the fluidity of photoreceptor outer segment disc membranes and optimize the environment for phototransduction (Agbaga et al, 2010; SanGiovanni and Chew, 2005; Litman et al., 2001). The beneficial effects of DHA extend beyond photoreceptor cells and have been reported to influence RPE cells as well. The RPE has a special role in modulating the level of DHA being delivered to photoreceptor outer segments (Bazan, 2009). A specialized task includes synthesizing a neuroprotective derivative of DHA, NPD1 (Bazan, 2009).

This derivative has been observed to inhibit pro-inflammatory events and acts as survival agent for the RPE and corresponding retinal neural tissue (Calandria & Bazan, 2010).

Recent literature suggests that incorporation of docosahexaenoic acid (DHA) in patients' diet has a beneficial effect in slowing the progression of macular degeneration (Ho et al, 2011). By employing questionnaires on dietary intakes of individuals both at risk for developing or already diagnosed with AMD, multiple research groups have consistently described a relationship between high DHA dietary intake and a slower disease progression or a reduced risk for developing AMD (Ho et al, 2011; Chiu et al, 2009; SanGiovanni et al 2008; Augood et al, 2008; Delcourt, 2007). The benefits of DHA extend towards patients with STGD3 as well. In the case study of a 15-year-old patient with STGD3, marked improvement in visual function were correlated with increased dietary DHA intake and vice versa (MacDonald et al, 2003). Yet another study indicated an inverse relationship between concentrations of omega-3 long chain fatty acids, EPA and DHA, in adipose and red blood cell membrane lipids with phenotype severity in a family affected by STGD3 (Hubbard et al, 2006). Healthy visual function and anatomy were related to dietary omega-3 fatty acid intake. A study conducted in the Sauvé lab show the same effect for DHA supplementation in the transgenic *ELOVL4* mice (Dornstauder et al, 2012). Retinal pigmented epithelium (RPE) and inner and outer retina function was preserved when DHA was supplied for at least 6 months. Additionally, lipofuscin accumulation in the

retina is reduced. Given these results, it is clear that DHA has a positive effect on the symptom severity of macular degeneration.

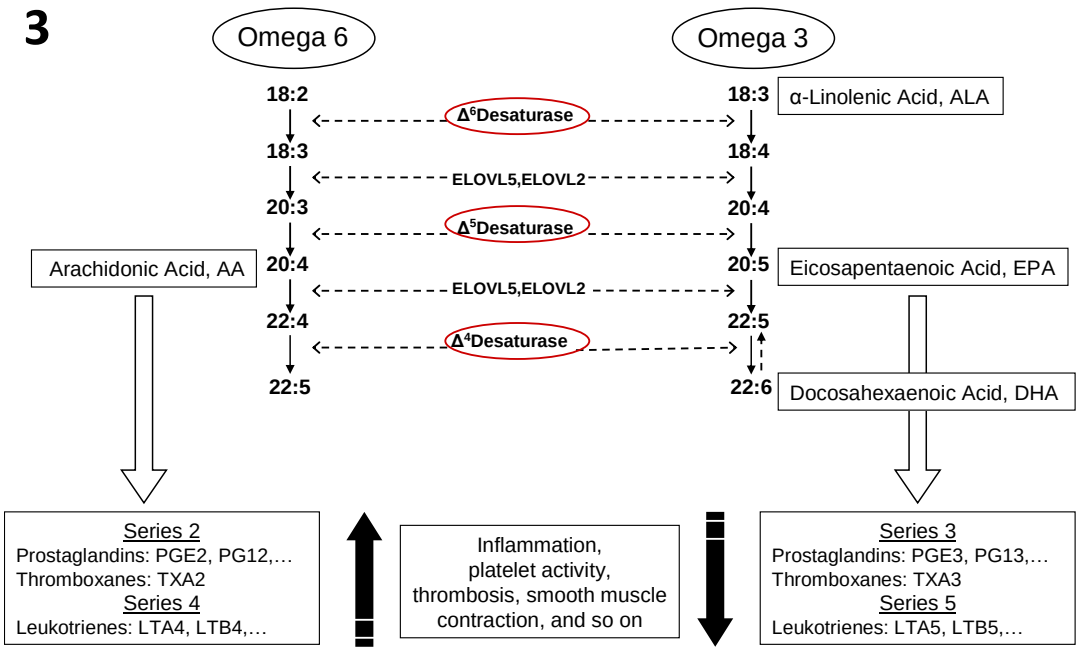


***Figure 3.*** **Pathways for omega-6 and omega-3 fatty acid metabolism**. Dietary intake of essential omega-6 and omega-3 fatty acids should be maintained at a balanced ratio for they share common enzymes in their metabolic pathway. Image from Querques et al, 2011.

### 1.4) Organization of the Retinal System

It is pertinent to be familiar with the structure and functional circuitry of the healthy retina to fully appreciate the mechanisms involved in retinal pathology. The neural retina maintains a stratified appearance due to the arrangement of various nerve and modulatory cells. Within the retinal tissue, 3 types of nerve cells exist. The photoreceptor, bipolar, and ganglion cells form 3 nuclear layers which, listed from the outermost to innermost layers, are referred to as the outer nuclear layer (ONL), inner nuclear layer (INL), and ganglion cell layer (GCL). Between these nuclear layers are the outer plexiform layer (OPL) and the inner plexiform layer (IPL) where synaptic connections occur. Additionally, horizontal and amacrine cells, forming tangential connections within the INL, are responsible for modulating neural inputs between nerve cells (Figure 4). And last, Müller cells, glial cells that act as supportive structures, span the entire thickness of the retina. Altogether these cells create the retina which is approximately 0.5 mm in thickness. It should be noted, however, that the thickness and cellular components vary across retinal eccentricity. The central region is cone dominant where subsequent one-to-one connections with corresponding bipolar and ganglion cells contribute to thicker inner nuclear and ganglion cell layers. Within the central retina also resides a specialized zone known as the macula. Containing solely cone photoreceptors, the macula is only 200 µm thick and is dedicated for detailed, colour vision. Incidentally, this area is the most vulnerable to injury; hence, the development of *macular* degeneration (webvision.med.utah.edu).

As mentioned previously, the pigmented epithelium and choroid are largely involved in visual function as well. The RPE and photoreceptor cells are dependent on each other for function and survival. Degeneration or mutation of one cell type has been reported to result in the secondary death of the other (Bhutto & Lutty et al, 2012) thus, the ability of photoreceptors to perform phototransduction relies heavily on the RPE. Its most obvious responsibility, based on its appearance, is light absorption. Melanin granules within the RPE provide its pigmentation and ability to absorb light, prevent light scatter, and improve the quality of vision. Aside from this vital role, the RPE has also been noted to renew light-damaged photoreceptor outer segments via phagocytosis on a daily basis. It contains enzymatic and non-enzymatic anti-oxidants to maintain defense mechanisms against photo-oxidation and ultimately, retinal structural integrity (Wang et al, 2006). Several other important responsibilities include participation in forming the blood retinal barrier, interaction with the choroid to nourish and supply oxygen to photoreceptors, and generation of 11-cis-retinal from all-trans-retinal to sustain phototransduction (webvision.med.utah.edu). The choroid works in conjunction with the RPE to appropriately supply the photoreceptors and other retinal cells with nutrients and oxygen. In mammals, 65-85% of blood is supplied via the choroid to nourish, predominantly, photoreceptors (Henkind et al., 1979). The other 15-35% of blood is supplied via the central retinal artery, which branches from the optic nerve and perfuses the inner retinal layers. A vasculature-free zone is formed in the peri-macula so as to provide a clear, direct path for photons to travel and reach cone photoreceptors.

The intricate interactions among the retinal vasculature, pigmented epithelium, and neural retina are imperative for visual function (Zhang, 1994). As a result, interference in any of these structures or their performance is likely to cause visual defects or vision loss.

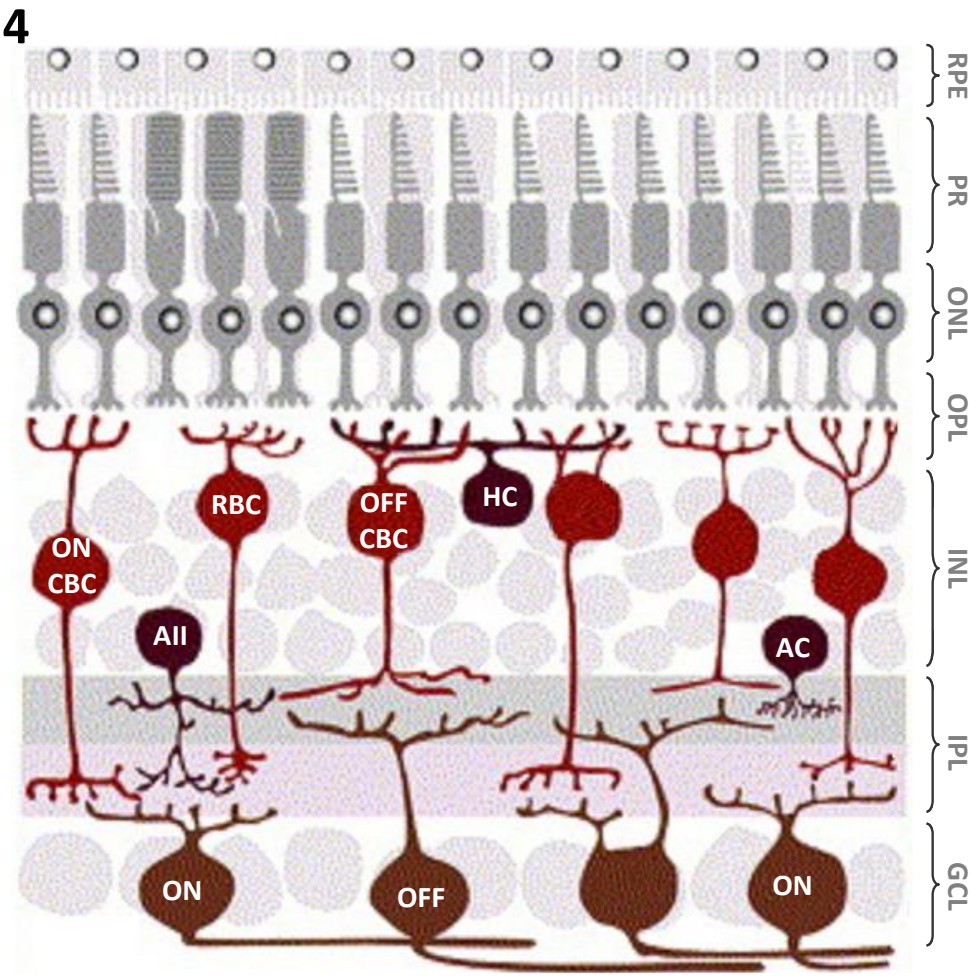


***Figure 4.*** **Cellular structure and synaptic connections of the retina.** In the outermost layer, the RPE makes direct contact with photoreceptors. The ONL, INL, and GCL comprise of nuclei from rod and cone photoreceptors, bipolar cells, and retinal ganglion cells, respectively. Synaptic connections between photoreceptor, bipolar, and horizontal cells occur in the OPL while bipolar, retinal ganglion, and amacrine cells connect in the IPL. AII amacrine cells unite rod bipolar cells with cone bipolar cells. Both ON and OFF bipolar and ganglion cells exists in the cone pathway. RPE, retinal pigmented epithelium; ONL, outer nuclear layer; OPL, outer plexiform layer; INL, inner nuclear layer; IPL, inner plexiform layer; GCL, ganglion cell layer; CBC, cone-drive bipolar cell; AII, AII amacrine cell; RBC, rod bipolar cell; HC, horizontal cell; AC, amacrine cell; ON/OFF, ON/OFF ganglion cell. Figure adapted from Tian (2004) *Visual experience and maturation of retinal synaptic pathways.*

### *1.4A) Rod-based Vision*

Under dim light conditions, vision is directed via rod-driven neurons in the retina. Though unable to detect fine detail, rod photoreceptors are highly sensitive to movement and are essential for navigation in dim light or scotopic conditions. Despite our dependence on detailed colour vision, human retinas consist primarily of rod and rod-associated neurons. The convergence of all these rod photoreceptors and corresponding nerve cells contributes to their movement detection property. Rod photoreceptors are perpetually depolarized and continuously release glutamate into the synaptic space under dark conditions. This activity is supported by a constant flow of ions known as the dark current (Figure 4). Cyclic nucleotide gated (CNG) channels maintain the flow of ions, but are disrupted with the absorption of a photon. First, a photon is captured, inducing a conformational change of 11-cis-retinal to all-trans-retinal within the rhodopsin (Figure 5A). The now enzymatically active rhodopsin can trigger a cascade of protein activation. Transducin, the G-protein, is first to be catalyzed which in turn activates phosphodiesterase (PDE). This will provoke hydrolyzation of cytosolic cyclic guanosine monophosphate (cGMP) into GMP (Figure 5B). Without the high concentration of cGMP required to maintain the cyclic nucleotide gated (CNG) channel open, these gates close and glutamate release is terminated. Once the phototransduction cascade occurs, roughly 15-30 rod photoreceptors transmit electrical information by converging to a single bipolar cell. All rod bipolar cells have inhibitory mGluR6 glutamate receptors and therefore respond to the interruption of glutamate release by depolarization (Vardi & Morigawa, 1997;

Nomura et al 1994). Before transmitting further information to ganglion cells, rod bipolar cells interact with various amacrine cells in the IPL. First, small-field AII amacrine cells connect rod bipolar cells to cone bipolar cells via gap junctions (Kolb & Famiglietti, 1974; Figure 3). Without the assistance of AII amacrine cells, scotopic vision would not be attained given that the rod pathway is void of a direct connection to ganglion cells. These amacrine cells allow rod bipolar cells to form connections with both ON-depolarizing and OFF-hyperpolarizing ganglion cells. Other amacrine cells known to assist in rod-driven vision are A17 cells. As many as 1000 rod bipolar cells can contact a solitary A17 amacrine cell. Because they do not contact other amacrine and ganglion cells and exclusively interconnects rod bipolar cells, A17 cells are also known as reciprocal amacrine cells (Hartveit, 1999). Considering their sensitivity to dim light, diffuse branching, and high convergence with rod bipolar cells, it is believed that A17 amacrine cells are responsible for amplifying and modifying the sensitivity of rod-driven vision (Menger et al, 2000; Nelson & Kolb, 1985). Finally, dopaminergic A18 amacrine cells participate in the ability for rod bipolar cells to connect with cone bipolar cells. Dopamine released from these cells disrupts the connection between AII amacrine and retinal bipolar cells and ultimately prevents signals from rod photoreceptors to reach ganglion cells (Mills & Massey, 1995). Circadian cycles influence the secretion of dopamine in A18 cells such that release is more pronounced in the morning under light conditions and more discrete in the evening under dim conditions (Krizaj, 2000). Following a multitude of interactions and communication with several types of amacrine cells,

rod bipolar cells are able to form an indirect connection to retinal ganglion cells and send scotopic information to the visual cortex.

**5**

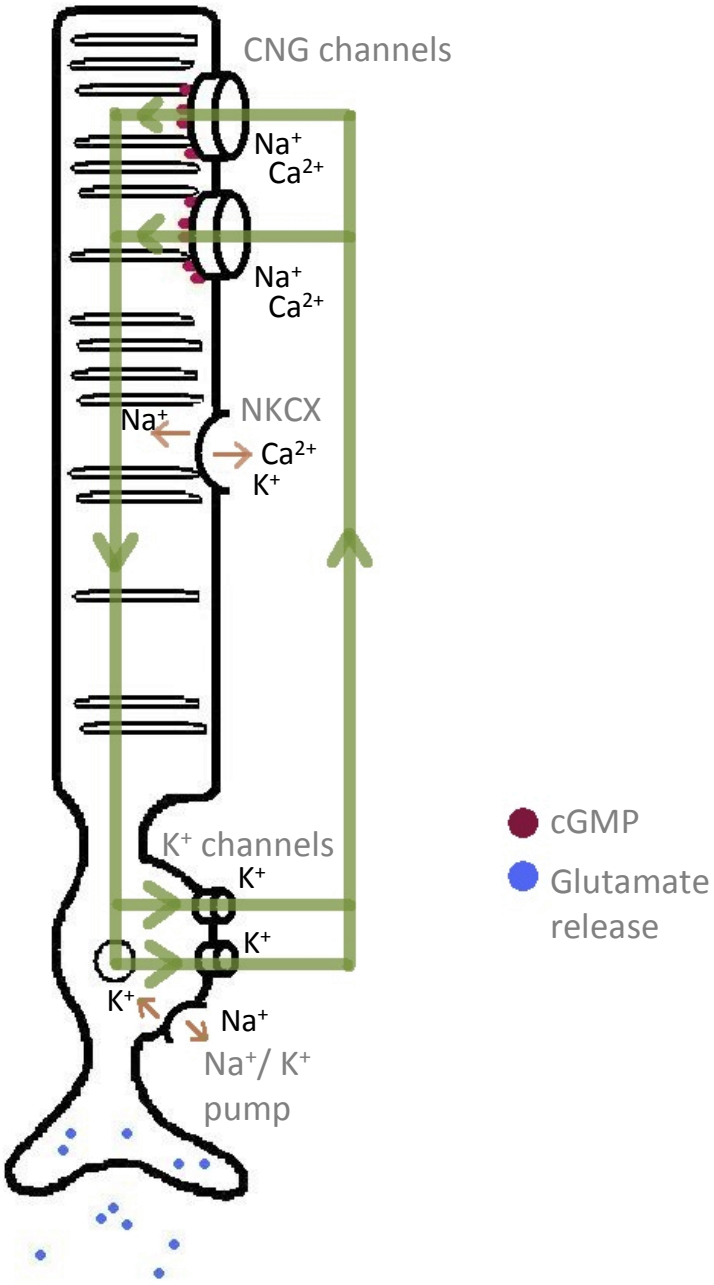


***Figure 5.*** **Dark current in rod photoreceptor.** Ion flow through the rod photoreceptor outer an inner segment is managed by multiple different channels and pumps. The dark current is disrupted when cGMP levels are reduced and CNG channels close. Illustrated channels are not proportional and displayed larger for demonstration purposes. CNG, cyclic nucleotide gated; NKCX, sodium potassium calcium exchanger.

6

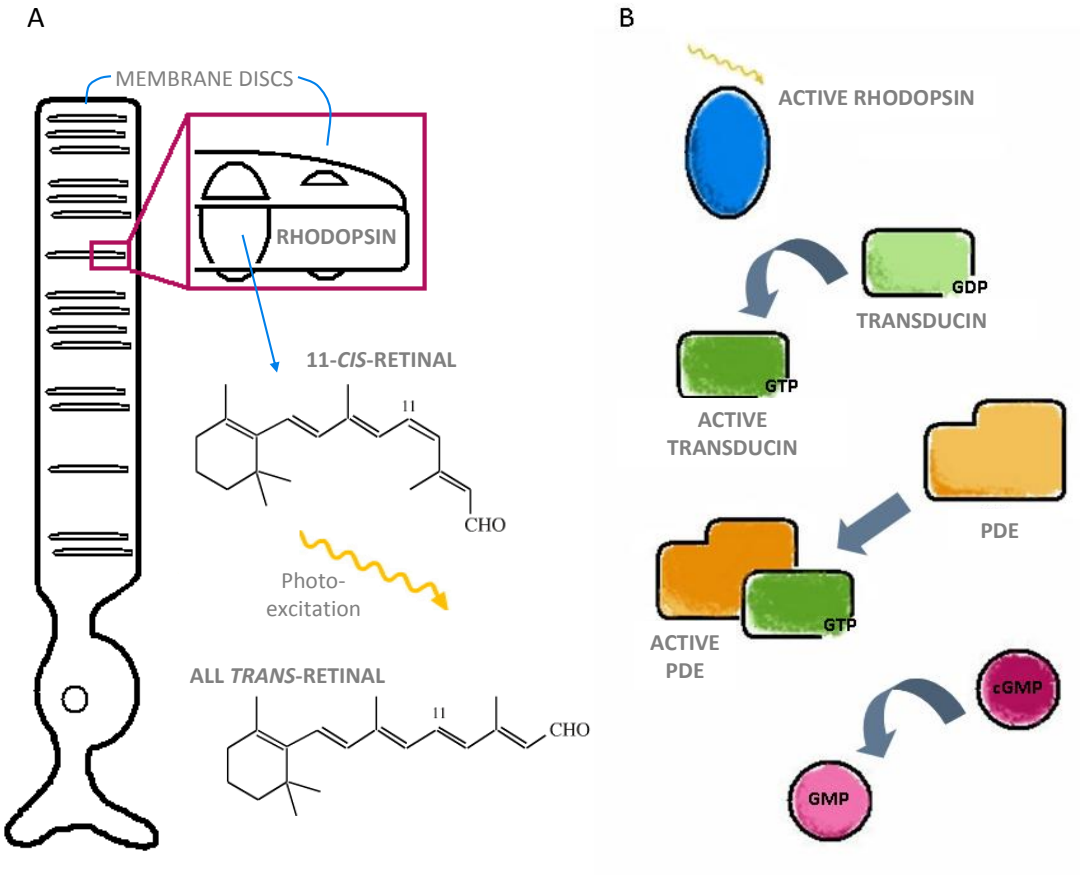


***Figure 6.*** **Phototransduction cascade.** (A) Membrane discs located in rod outer segments contain rhodopsin which are light sensitive. Upon light detection, 11-cis-retinal within the rhodopsin photo-isomerizes into all-trans-retinal and elicits a series of protein activation. (B) The G-protein, Transducin, responds to the active rhodopsin and becomes activated, converting PDE into its active form. cGMP is hydrolyzed into GMP.

### *1.4B) Cone-based Vision*

Our ability to perceive vibrant colours in fine detail under bright or flickering light conditions relies on our cone system. Cone-based vision differs from rod-based vision in several aspects. Differences are already detected at the level of cone photoreceptors. Unlike rod photoreceptors, cone outer segment plasma membranes do not form discrete, free-floating disks. Instead, invaginations from plasma membranes enhance cone outer segment surface area (Michaelides et al, 2006). Cones also exist in various forms depending on the visual pigments and opsins found within their outer segments. The sensitivity of visual pigments to specific wavelengths of light is what provides us with colour vision (Westheimer, 1984). Red, green, and blue colour perception is derived from the ability of these photoreceptors to detect long, medium, and short wavelengths, respectively. Furthermore, the cone pathway consists of more than one kind of bipolar cell. What differs amongst these cone bipolar cells are the size of their dendritic field, type of their synaptic contacts, and response of their glutamate receptors. In contrast to rod bipolar cells, these cells make direct contact with ganglion cells. They do not rely on AII amacrine cells. One final distinguishing feature of the cone system is its ability to produce high acuity vision and detect contrast. A lower convergence from photoreceptors to bipolar to ganglion cells allows for high acuity vision (with reduced sensitivity to motion), while their relationship between horizontal cells and cone photoreceptors in the OPL contributes to contrast detection. Horizontal cells act to discern foreground and background by muting signals detected from surrounding edges. Detailed

information from cone bipolar cells are transmitted to ganglion cells before arriving in the visual cortex.

**1.5) Electroretinography**

ERGs are frequently employed to measure response activity from specific nerve cells within the retina. Lights of different intensities are flashed before the subject to elicit membrane hyperpolarizations and post-photoreceptor depolarizations within the retinal tissue. These membrane potentials are then recorded via conducting electrodes placed on the cornea. In this instance, membrane potential (voltage, V) is derived from ionic refluxes (current, I) traveling along retinal and ocular tissues which act as resistors (resistance, R) as illustrated in Figure 7 (webvision.med.utah.edu). Generated waveforms display 2 distinctive peaks: a negative a-wave and a positive b-wave. The a- wave, which precedes the latter, represents hyperpolarizing photoreceptor activities while the b-wave signifies bipolar cell depolarization. A-wave amplitudes are measured from the baseline to the trough of its negative peak. Conversely, b-waves are measured from the trough of the a-wave to the apex of it own peak. The time required to elicit these waves, known as implicit time, is determined from the onset of light stimulation to the peak of the respective wave (Figure 8A). Generally, amplitude reveals the quantity of responding cells and implicit time displays their biochemical integrity. Furthermore, the nature of the ERG protocol can be manipulated by altering the brightness and frequency of light stimulation. Background illumination can be offered to obtain photopic, cone-dependent

responses. Otherwise, dimly lit conditions can be used to obtain rod-dependent responses. By altering the frequency of flashes, one can observe the recovery rate or even the efficiency of the phototransduction cascade. Thus, the ERG is an invaluable instrument for detecting changes in specific mechanisms of the retinal visual system.

**7**

A

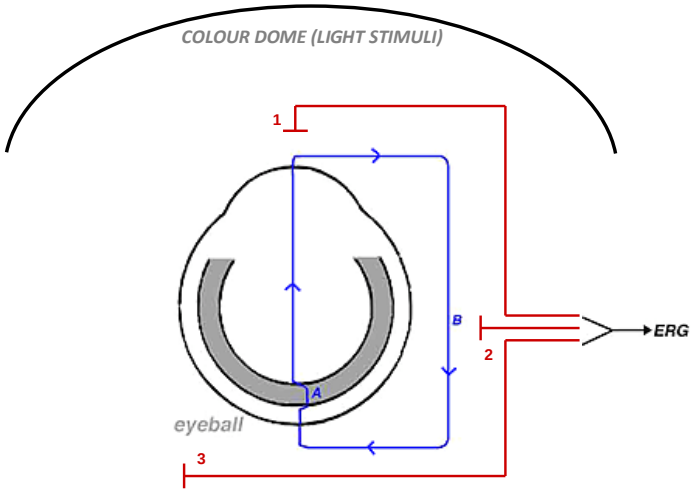


B

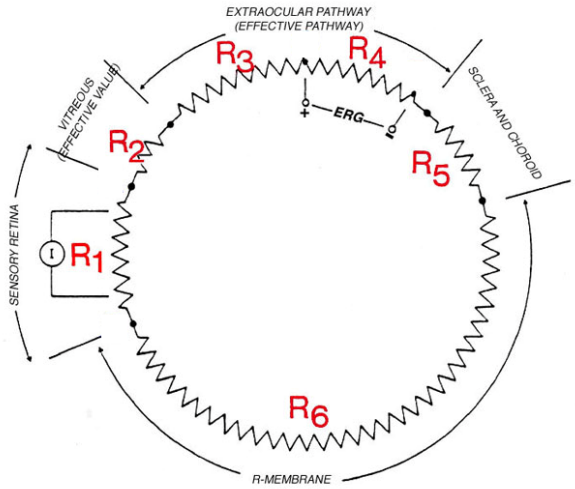


***Figure 7.*** **ERG circuitry.** (A) Extracellular currents are amplified and recorded by the ERG. A light stimulus elicits current flow within the retina, pathway A, which is transmitted through the vitreous and cornea, pathway B. A recording electrode, 1, picks up this activity via the cornea. A reference, 2, and ground electrode, 3, are placed between the eye and the ear and between the ears, respectively. (B) Several tissues offer resistance through which current flow. Current in pathway A flow through $R_1$, while pathway B flows through $R_{2\text{-}6}$. $R_1$, sensory retina; $R_2$, vitreous; $R_3$, extraocular pathway, $R_4$, ERG recording electrode; $R_5$, sclera and choroid, $R_6$, retinal epithelium. Images adapted from http://webvision.med.utah.edu.

8

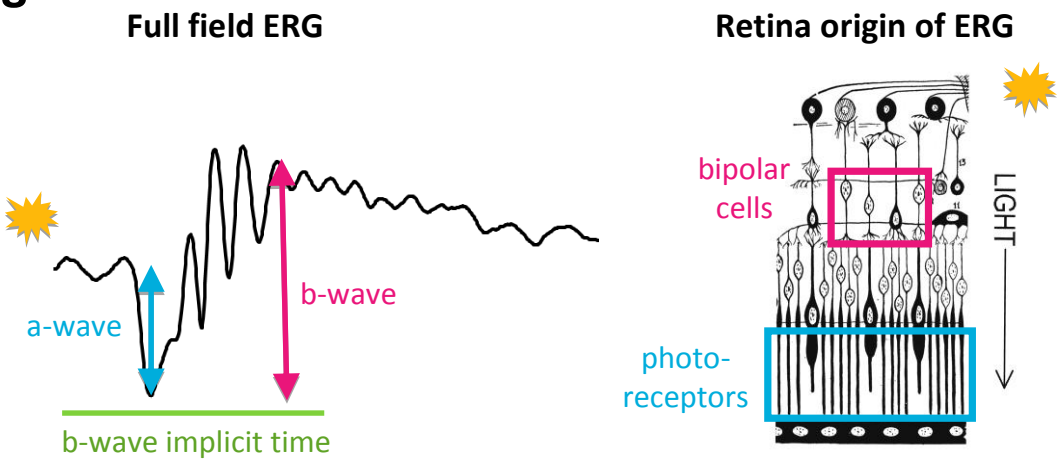


***Figure 8.*** **Origins and components of ERG traces.** a-wave amplitudes, measured from the baseline to the trough, correspond to photoreceptor integrity. Conversely, b-wave amplitudes are measured from the trough of the a-wave to the peak of the positive wave and represent bipolar cell activity. Implicit time is measured from the onset of the light stimulus and demonstrates the biochemical activity of the corresponding peak from which it is measured to.

## Chapter 2. RESEARCH PLAN

### 2.1) Rationale

The transgenic *ELOVL4* mouse model shares many similarities with human STDG3 and dry AMD pathology. Lipofuscin accumulation, reduced ERG responses, and abnormal fundus morphology (Dornstauder et al, 2012) renders this model an exceptional tool to study the mechanisms or effects of altered fatty acids on visual function. Though it has been established that omega 3 fatty acids are abundant in retina, brain, and testis (Agbaga, 2010), their role in retinal health and pathology is poorly understood. The use of this model has the potential to elucidate the influence of these fatty acids on retinal degeneration. An added benefit is the rate of retinal disease progression of this animal model as compared to human STGD3 and AMD pathology. Neither being too rapid nor too slow, the progression of retinal degeneration in this animal model offers an ideal window for therapeutic intervention.

So, why select DHA supplementation as a method of therapeutic intervention? Consistent findings reveal reduced risk for developing AMD or slowed disease progression in individuals or patients, respectively, with higher levels of DHA in blood plasma levels. (Ho et al, 2011; Chiu et al, 2009; SanGiovanni et al 2008; Augood et al, 2008). Evidence of the beneficial effects of DHA dietary supplementation was reported in patients affected by STGD3 as well (MacDonald et al, 2003; Hubbard et al, 2006). A study conducted in our lab showed that DHA supplementation was associated with preserved RPE as well as inner and outer retina function in the transgenic *ELOVL4* mouse model of

STDG3. Additionally, lipofuscin accumulation in the retina was also reduced (Dornstauder et al, 2012). Overall, the results mentioned above support the proposition that DHA might act as an effective therapeutic intervention. Being only 22 carbon chains long, DHA is not directly related to the ELOVL4 protein, which functions to elongate very long chain fatty acids of at least 28 carbon chains. However, it is very possible that it interacts with the omega 3 VLCPUFA typically generated from ELOVL4 elongases. Of note, both species are found in high proportion in the retina and contribute the structural integrity of photoreceptors.

The benefits of DHA supplementation have already been outlined, but it has yet to be discovered how it might affect retinal degeneration if supplied during development *in utero.* Early changes in protein and gene expression in *ELOVL4* mice have been discovered at 1 month (Kuny et al, 2012), suggesting an advantage to begin dietary intervention before this time point. By providing the diet antenatally, there is more time for DHA to accumulate in the retina and influence mechanisms involved in retinal degeneration. Accretion of DHA may also potentiate the beneficial effects already observed in mice supplemented at 1 month of age. Smithers et al, 2008 demonstrated that visual acuity of neonates is vastly improved when supplementation with DHA is provided during critical developmental stages.

## 2.2) Hypothesis

I propose that antenatal dietary supplementation of the omega-3 fatty acid docosahexaenoic acid will prevent deterioration of visual function in transgenic mice expressing a gene related to macular degeneration by maintaining a healthy level of DHA in retinal tissue. This statement implies that antenatal DHA supplementation will:

1) Maintain retinal responsiveness as indicated by preserved amplitudes of ERG a- and b-waves
2) Maintain photoreceptor numbers
3) Result in higher retina DHA level compared to non-supplemented animals.

## 2.3) Objectives

A main goal of this study is to investigate how DHA accretion might affect the lipid environment of photoreceptors in a manner that leads to reduced progression of retinal degeneration. To fulfill this objective, we will examine the impact of dietary DHA supplementation on retinal function, photoreceptor survival, and fatty acid content in the retina of healthy and diseased animals (ELOVL4 mouse model of STGD3). The premise of providing DHA antenatally is to 1) offer precocious intervention on the degenerative events of the disease, which are already detectable by 1 month of age (Kuny et al., 2012); and 2) supply insights on how DHA supplementation might influence retinal development in an animal model of retinal degeneration.

## Chapter 3. EXPERIMENTAL DESIGN AND METHODS

### 3.1) Experimental Design

#### *3.1A) Animals*

The experimental study was performed on the offspring of heterozygous *ELOVL4/TG1-2* (TG) and wild-type (WT) C57Bl/6n mice (Charles River Laboratories, Wilmington, MA) from an *ELOVL4/TG2* colony initially maintained the laboratory of Dr. Kang Zhang (Karan et al., 2005) and later sustained at the University of Alberta. In every case, WT female mice were paired with TG males. DNA extracted from ear notches of these breeders and their litters was collected to determine their genotypes by employing polymerase chain reaction (PCR) and using *Elovl4* primers 5'-TGTAGCAGACTGGCCGCTGAT-3' (forward) and 5'-CTCTGAAGATGAAAAGGTTAAGCA-3' (reverse) and *ELOVL4* primers 5'-GCAGTCTCCTTGGCCTACAC-3' (forward) and 5'-GAATTCAACTGGGCTCCAAA-3' (reverse). To promote breeding between mating pairs, cages were provided with large aspen shavings, krinkle paper, and a single nesting sheet and finally, aspen chips and PVC tubes were replaced with SoftZorb (Paper-Based Laboratory Animal Bedding, Northeastern Products, Corp., Warrensburg, NY, USA) and paper huts, respectively. Pups were then maintained in standard housing conditions with small aspen chips and PVC tubes upon weaning at 3 weeks of age. All animals were housed in polycarbonate cages with food and water provided *ad libitum* in an environment with humidity and temperature of 50% and 21$^{o}$C, respectively. Knowing that production of IRBP mRNA is affected by circadian rhythm, all animals were exposed to a 12:12 light-

dark cycle to ensure adequate expression of the *ELOVL4* gene. Experiments were carried out in accordance with the Institutional Animal Care and Use Committee (University of Alberta; license #463) and the ARVO (Association for Research in Vision and Ophthalmology) Statement for the Use of Animals in Ophthalmic and Visual Research.

### *3.1B) Dietary Manipulation*

Mice were provided 1 of 3 diets in this study. One diet was a standard laboratory chow (Laboratory Rodent Diet #5001 LabDiet; Nutrition International, Richmond, IN) and the other two were custom-made semi-purified diets. Serving as a control, the laboratory chow represents the typical consumption of DHA and contains 0.19 % omega-3 fatty acid. The two custom diets served as a negative control diet containing 0% DHA and a test diet containing 2% w/w DHA of total fat (Table 1 and 2). All diets were nutritionally complete. Chow fed animals received 28.5% protein, 13.5% fat, and 56.0% carbohydrates of their caloric intake while the other diets consisted of 30.7% protein, 20.7% fat, and 48.6% carbohydrates. Custom made diets were prepared monthly, stored at -20$^{o}$C, and replaced in clean food jars (Unifab Corp., Kalamazoo, MI, USA) 3 times a week. These procedures were implemented to prevent ingredients from oxidizing and to ensure mice were receiving a stable concentration of all nutrients. All diets were commenced antenatally by providing breeding pairs their respective diets the first day they were matched. Four mating pairs were fed chow, 5 were fed DHA-, and 7 were fed DHA+. This produced 6 experimental groups: i) chow fed WT mice

(WT chow, n=10); ii) chow fed TG mice (TG chow, n=12); iii) DHA deficient WT mice (WT-, n=14); iv) DHA deficient TG mice (TG-, n=24); v) DHA supplemented WT mice (WT+, n=24); and vi) DHA supplemented TG mice (TG+, n=22).

**Table 1: Composition of custom-made diets**

| Ingredients | DHA- (g/kg) | DHA+ (g/kg) |
|---|---|---|
| *Basal* | | |
| Casein | 270.00 | 270.00 |
| L-Methionine | 2.50 | 2.50 |
| Dextrose monohydrate | 208.49 | 208.49 |
| Corn starch | 200.00 | 200.00 |
| Cellulose | 50.00 | 50.00 |
| Mineral mixture | 50.85 | 50.85 |
| Sodium Selenite | 0.30 | 0.30 |
| Manganese Sulfate | 0.24 | 0.24 |
| Vitamin mixture (AOAC) | 10.00 | 10.00 |
| Inositol | 6.25 | 6.25 |
| Choline Chloride | 1.38 | 1.38 |
| *Fat Blend* | | |
| Olive oil | 45.0 | 59.0 |
| Canola oil | 68.0 | 50.0 |
| Coconut oil | 42.0 | 42.0 |
| Corn oil | 44.0 | 44.0 |
| Docosahexanoic acid oil | 0.0 | 5.0 |

The basal mixture is a Teklad Custom Research Diet (TD.84172) purchased from Harlan Laboratories (Madison, WI, USA)
* Bemhart-Tomarelli (170750)
** No. 40055, A.O.A.C., Association of Analytical Communities (http://www.aoac.org/)
*** Docosahexaenoic acid oil is DHASCO, an oil extracted from the unicellular alga *Crypthecodinium cohnii* that is mixed with high oleic sunflower oil (HOSO). DHASCO contains 46% DHA and 44% oleic acid.

**Table 2: Fatty acid composition of custom-made diets**

| Fatty Acids | DHA- | DHA+ |
|---|---|---|
| Caprilic Acid, C8:0 | 0.6 | 1.9 |
| Capric Acid, C10:0 | 1.5 | 1.9 |
| Lauric Acid; C12:0 | 13.8 | 14.5 |
| Miristic Acid, C14:0 | 5.1 | 5.9 |
| Tetradecenoylcarnitine, C14:1 | 0 | 0 |
| Palmitic Acid, C16:0 | 9.8 | 10.5 |
| cis-7 hexadecenoic acid, C16:1 n9 | 0.6 | 0.7 |
| Stearic Acid, C18:0 | 2.2 | 2.1 |
| Vaccenic Acid, C18:1 t11 | 0.6 | 0 |
| Oleic Acid, C18:1 n9 | 37.2 | 35.4 |
| Ceramide, C18:1 c1 | 2.0 | 1.2 |
| Linoleic Acid, C18:2 n6 | 21.8 | 20.7 |
| Linolenic Acid. C18:3 n3 | 0.3 | 0.3 |
| Arachidic Acid, C20:0 | 2.9 | 2.3 |
| Eicosadienoic Acid, 20:2 n6 | 0 | 0 |
| Di-homo-gamma-linolenic Acid, C20:3 n6 | 0 | 0 |
| Arachidonic Acid; C20:4 n6 | 0 | 0 |
| Eicosapentaenoic Acid, C20:5 n3 | 0 | 0 |
| Adrenic Acid. C22:4 n6 | 0 | 0 |
| Docosapentaenoic Acid, C22:5 n3 | 0 | 0 |
| ***Docosahexaenoic Acid, C22:6 n3*** | ***0*** | ***1.9*** |
| | | |
| Total Saturated Fatty Acids | 33.3 | 37.1 |
| Total Mono-unsaturated Fatty Acids | 40.4 | 37.2 |
| Total Poly-unsaturated Fatty Acids | 24.7 | 24.9 |
| Total Omega-3 | 2.9 | 4.2 |

### *3.1C) Tissue Collection*

The experimental period ended at 3 months of age, when mice received an intraperitoneal injection of 0.5 mL of Euthanyl (Bimeda-MTC Animal Health Inc, Cambridge, ON, Canada) followed by cervical dislocation. After assurance that the animals were deceased (by the lack of toe-pinch response), both eyes were enucleated and ocular tissues collected.

## 3.2) Experimental Methods:

### *3.2A) Electroretinogram (ERG) Recordings*

Retinal function was assessed longitudinally at 1 and 3 month time points among the 6 experimental groups using the full-field ERG. Prior to recording ERGs, animals were anaesthetized with a mixture of 5:1 ketamine (Ketalean, Bimeda-MTC Animal Health, Inc., Cambridge, ONT, Canada): xylazine (X1251, Sigma-Aldrich Co., St. Louis, MO, USA) (75 mg/kg: 15 mg/kg, respectively) via intraperitoneal injection with a 26 gauge needle (0.45mm x 13 mm, PrecisionGlide Needle, Becton Dickinson & C., Franklin Lakes, NJ, USA). The anaesthesia provides analgesia and muscle relaxation, but also causes hypothermia. To counter this effect, a homoeothermic electrical blanket was used to maintain animal body temperatures at $38^{o}$C.

After 10-15 minutes, when animals were completely anaesthetized (indicated by lack of righting reflex), active gold recording electrodes were placed on both corneas, 25 gauge platinum reference electrodes were placed subdermally behind each eye, and a single 25 gauge platinum ground electrode was inserted in

the scruff. Pupil dilation and corneal lubrication was then achieved using 1% tropicamide eye drops and 0.3% hypromellose (GenTeal Gel, Novartis Ophthalmics, Novartis Pharmaceuticals Canada Inc., Mississauga, ON, Canada), respectively. These also served as conducting fluid, connecting the corneal surface with the recording electrodes.

Visually elicited mass potentials from the retina were recorded using the Espion E2 system (Diagnosys LLC, Littleton, MA, USA). Light stimulation, signal amplification (0.3 -300 Hz bandpass), and data acquisition are all offered by this system. Specific combinations of light intensity and frequency of stimulation are created to reveal information on retinal nerve cell activity. For instance, rod and cone photoreceptor activity can be assessed using scotopic and photopic intensity response protocols, respectively.

Scotopic intensity response tests were ideal for identifying responses from both rod and cones photoreceptors. This protocol required mice to be dark adapted for at least 1 hour before proceeding with ERG tests. Once ready, single white flashes of light (6500 K Xenon bulb at 10 μs duration) were presented in 19 steps at increasing intensities from -5.22 to 2.86 log cds/$m^2$. Each step was repeated 3-5 times to confirm response consistency and retrieve averages. Additionally, inter-stimulus intervals were spaced according to stimulus intensity, with 10 sec between the first few low intensity flashes leading up to 60 sec between the highest intensity flashes. This was done to allow sufficient time for rod photoreceptor recovery.

Photopic intensity response tests were performed in a similar fashion as scotopic tests. In this case, a background illumination of 30cds/$m^2$ was present as light stimulation was flashed in 11 steps of incremental intensities ranging from -1.62 to 2.86 log cds/$m^2$. The duration, repetition, and inter-stimulus intervals of flashes were the same as previously described.

For all ERG tests, only the eye corresponding to the highest maximal dark-adapted a-wave amplitude was selected for statistical analysis.

### *3.2B) Retina Cross-sectional Staining*

To assess any differences in photoreceptor survival among the groups (n=8 for each experimental group), retinal eyecups were studied using stained cross-sections at 3 months. Mice were enucleated, with a portion of the optic nerve remaining attached to the eye, following euthanasia. Eyes were then placed in a Petri dish containing phosphate buffered saline (PBS, pH ~7.3) where the cornea was pierced with a scalpel (surgical blade stainless, No.11, Feather Safety Razor Co. LTD, Osaka, Japan). The eye was then placed in 4% paraformaldehyde (PFA) for 1 hour at 4$^o$C, after which point the cornea and lens were removed. To prevent damages to the retina, care was taken to avoid cutting beyond the boundaries of the limbus and injuring the ora serrata. The resulting eyecups were then subjected to a sucrose gradient treatment, beginning with 10%, followed by 20% sucrose exposure for 1 hour, and concluding with a 30% sucrose exposure overnight at 4$^o$C. Before the tissue was embedded, it was rinsed in resin (Tissue-Tek O.C.T. Compound, Sakura Finetek, Torrance, CA, USA) once to remove

excess sucrose and placed in a plastic cryomold. Enough resin was applied to engulf the entire eyecup prior to flash freezing with liquid nitrogen and subsequent storage in -80$^{o}$C.

The cryostat (Leica CM1850, Germany) was set at -25$^{o}$C to achieve the optimal temperature to perform cryosectioning. Cross sections were cut at 20µm thickness through the optic nerve, parallel to the temporal-nasal axis, and mounted on frosted glass slides (Superfrost plus, cat. no. 12-550-15, Fisher Scientific, USA). To ensure equal treatment between genotypes and prevent bias, 8-10 sections of both WT and TG animals were mounted on a single slide without providing genotype identities. As an additional precaution, 8 slides were prepared for each animal to allow for a wider selection. These were all stored in -20$^{o}$C for a minimum of 24 hours before staining.

Mounted slides were laid flat as they reached 20$^{o}$C. Once they reached room temperature, slides were washed in PBS in a glass coplin jar for 5 minutes. Any excess PBS was wicked off, 3-4 drops of anti-fade mounting media (Prolong Gold, Cat. #P36931; Molecular Probes, Eugene, OR, USA) containing 4, 6-diamidino-2-phenylindole (DAPI) was applied, and a glass coverslip (Microscope Cover Glass, 22x50, cat.no. 12-545E, Fisher Scientific, USA) was laid over the tissue before imaging. To provide sufficient time for slides to cure, they were laid flat overnight and sealed with clear nail polish.

Images were captured on a Zeiss LSM510 confocal microscope using a Plan-Neofluar 40x/1.3 oil objective. Because the DAPI within the mounting media is a fluorescent stain that binds to deoxyribonucleic acids (DNA), a

blue/cyan DAPI filter was used to assist in identifying the outer and inner nuclear layers. The most representative section containing the optic nerve head was selected for each animal and 3 images from this section were taken. These 3 images corresponded to the center (adjacent to the optic nerve), the periphery (adjacent to the ora serrata), and the middle (a location equidistant from the center and periphery) of the retina (Figure 9).

Images were first converted to 8-bit on ImageJ software before nuclear cell numbers were counted. A line, using the straight line tool, was placed across the length of the outer nuclear layer (ONL) and dots, using the paintbrush tool, was used to mark and count nuclei that contacted the line. This procedure was repeated 3 times for each image, counting cells in the middle and 0.5 - 0.75 inches away from either edges of the window (Figure 9). To confirm reliability and account for any subjectivity and that may be involved in the counting process, two separate evaluators performed the photoreceptor counts on the same cross-section images. Averages made from ONL numbers were obtained for all eccentricities and gathered for statistical analysis.

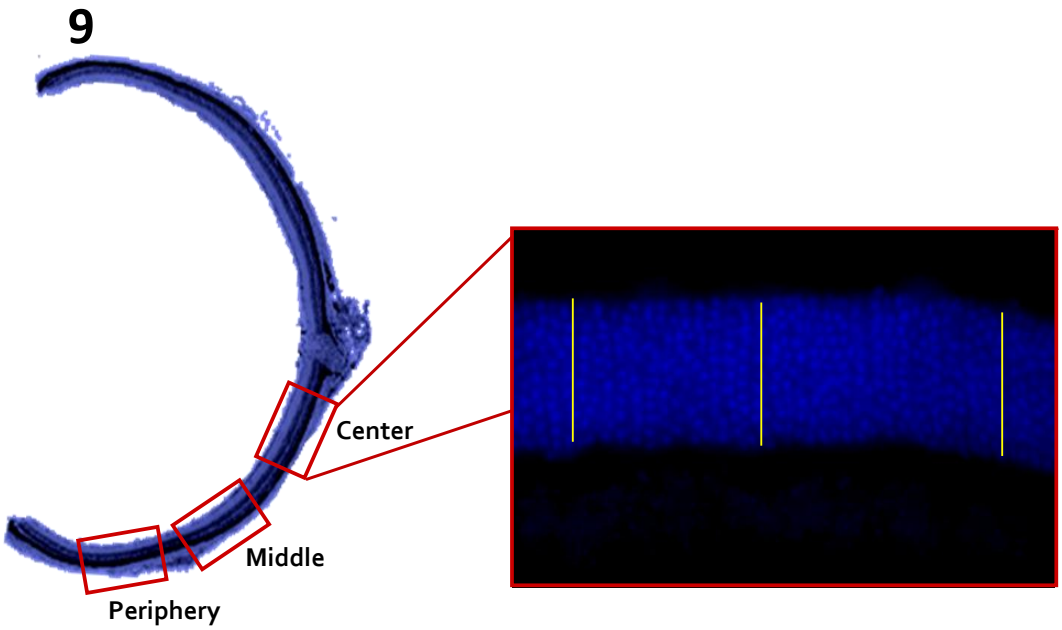


***Figure 9.*** **Cross-sectional photoreceptor counts.** Three counts of photoreceptor nuclei are made within each window of images taken from the center, middle, and periphery of the retina. All images are captured at 40x magnification using a fluorescent microscope.

### *3.2C) Retinal Fatty Acid Profile*

Fatty acid measures were conducted to compare the concentration of DHA in the retina to the therapeutic effects it might have on macular degeneration. First, eyes were collected and placed in PBS (pH ~7.3) in preparation for retina extraction. In the same manner as described in *Photoreceptor Cross-sectional Staining*, the cornea was excised and the lens removed. The resulting eyecup was inverted gently, making it easier to extract the exposed neural retina tissue. Retinas were flash frozen in 2 mL Eppendorf tubes

(Standard Micro Test Tube 3810X, Eppendorf Canada Ltd., ONT, Canada) and stored in -80$^{o}$C.

To extract lipids from retinal tissue, each individual retina was homogenized with 0.025% $CaCl_2$. The homogenate was then combined with 5mL chloroform: methanol (2:1) mixture, centrifuged at 350 x g for 12 minutes and stored in 4$^{o}$C overnight. The lower phase of the two newly formed layers were transferred to a tube and dried down in a water bath (30-40$^{o}$C) under nitrogen gas (Analytical Nitrogen Evaporator, N-EVAP 111, Organomation Associates, Inc, Berlin, MA, USA). After several washes with chloroform: methanol, further evaporation under nitrogen gas, and overnight storage in -20$^{o}$C the samples were ready for thin layer chromatography.

Phospholipids were separated on Analtech silica-gel G thin-layer chromatography plates (20x20 μm, cat. no. 01011, Mandel Scientific Co., Guelph, Ontario, Canada) with petroleum ether/diethyl ether/acetic acid (80:20:1, v/v/v) as the solvent system. To visualize phospholipid bands, 0.1% analine naphthalene sulfonic acid in water (ANSA, w/v) were sprayed on each plate and imaged under UV light. Marked bands were scraped into vials and processed into fatty acid methyl esters using a $BF_3$/haxane reagent. Double distilled water was added to methylated samples and centrifuged for 12 minutes at 350 x g (1300 rpm). The extracted upper phase was then washed and dried down repeatedly with hexane and nitrogen gas, respectively.

Automated gas-liquid chromatography (Vista 6010 G.L.C. and Vista 402 data system; Varian Instruments, Mississauga, Ontario, Canada) separated the

components of the remaining sample. Chromatography was performed using a fused silica BP20 capillary column (25m X 0.24mm i.d.; Varian, Mississauga, Ontario, Canada). Helium was used as the carrier gas at a flow rate of 1.8ml/minutes using a splitless injection mode. The initial oven temperature was 150°C, then increased to 190°C at 20°C/minute and held for 23 minutes, then increased to 220°C at 2°C/minute for a total analysis time of 40 minutes. These analytical conditions separated all saturated, mono-, di- and polyunsaturated fatty acids from $C_{12}$ to $C_{36}$ in chain length.

Resulting chromatographs and data were transferred into Excel spreadsheets to begin analysis. All relevant fatty acid peaks were selected and compared among all experimental groups (n=3-9 for each group) based on the percentage of peak area out of the total area. The adjusted total was then prepared for statistical analysis.

Inconsistencies in handling fatty acid samples between each trial yielded variable results. For this reason, only groups that were subjected to the same trial conditions were selected for statistical comparison and the chow fed groups were eliminated.

### *3.2D) Statistical Analysis*

A generalized linear regression model was used to analyze the potential effects of genotype and diet on ERG function with SPSS (IBM SPSS statistical software). Steps 10-18 of the scotopic tests were selected for analysis because differences among the experimental groups were not observed before step 10 and

because these responses resembled a linear formula. Under light conditions, only steps 7-11 elicited recognizable wave amplitudes and were, hence, selected for analysis. All ERG values were expressed as mean ± standard error of the mean (SEM).

To compare the effects of genotype on photoreceptors numbers and levels of AA or DHA, a two-way analysis of variance (ANOVA) tests was performed using Graphpad Prism 5 software. Considering the difference in variability between WT and TG groups, one-way ANOVA (non-parametric, Kruskal-Wallis, Dunn's Multiple Comparison test) and non-parametric, Mann-Whitney U-tests were performed within each genotype to assess the effects of diet on photoreceptor numbers and FA profiles, respectively. All values were expressed as mean ± standard error mean (SEM).

# Chapter 4. RESULTS

## 4.1) Function

### *4.1A) Scotopic Intensity Response (SIR)*

Recordings were performed longitudinally at both 1 and 3 months of age to detect potential early changes in retinal function between groups and to observe any modifications in retinal function over time. Compared to 1 month recordings (Figure 10), a and b wave amplitudes were lower and b wave implicit times increased slightly. This observation was true regardless of genotype or diet.

There was a statistically significant difference between WT and TG animals in regards to a-wave amplitudes, which were lower in TG, at both time points ($p<0.001$ at 1 month and $p<0.001$ at 3 months, Figure 10B and 11B). This distinction was more pronounced as stimulus intensity increased. Genotype differences in b-wave amplitudes existed as well, but only at 3 months ($p<0.05$). Implicit time, on the other hand, demonstrated no such differences between WT and TG animals for both a- and b-waves (Figure 10C and 11C). Retinal dysfunction has been previously reported in this line of TG animals (Dornstauder et al, 2012), however, 1 month a-wave amplitude reductions are the earliest detection of functional differences between TG and WT animals.

Diet had no observable effects on retinal function at 1 month (Figure 10B), however chow fed WT mice displayed reduced a- and b-wave amplitudes at 3 months ($p=0.007$ for a-wave and $p=0.02$ for b-wave, Figure 11B). B-wave amplitudes of these Chow fed WT animals behaved similarly to those of TG

animals. Again, it was more pronounced as stimulus intensity increased. Implicit time was, again, unaffected by dietary manipulation.

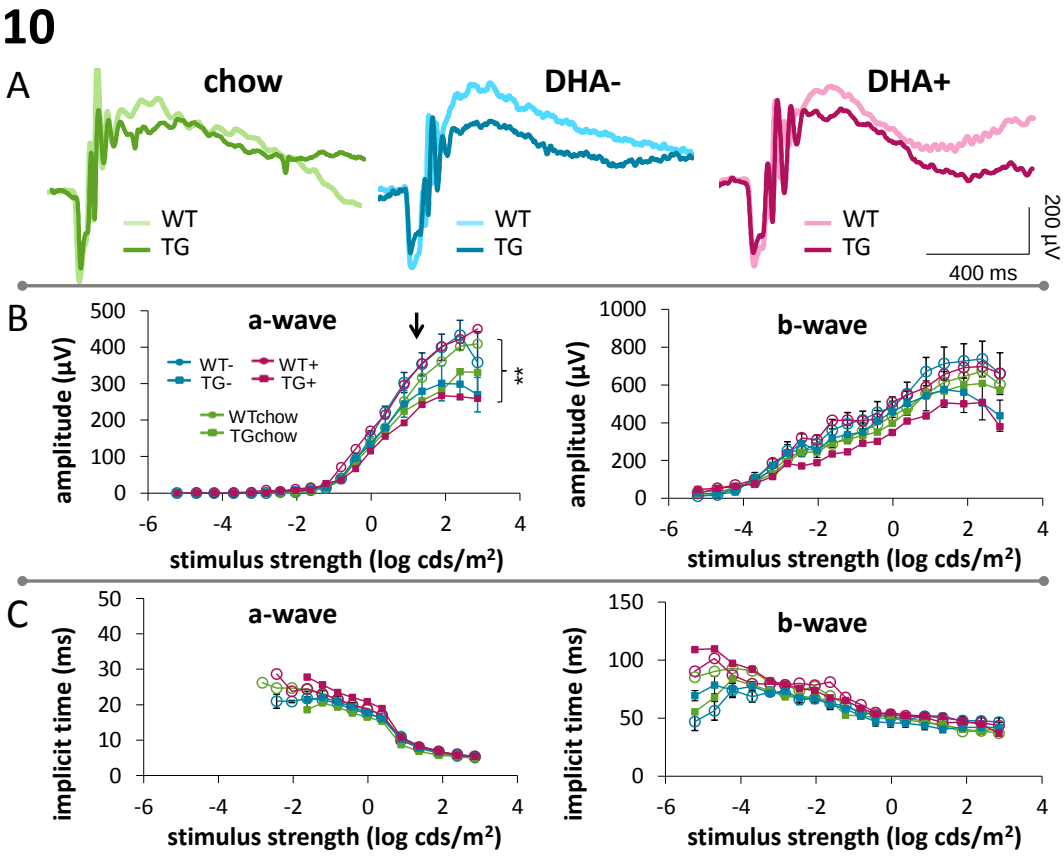


***Figure 10.*** **Scotopic intensity response at 1 month**. All data expressed as mean (A) Representative ERG traces at a stimulus intensity of 1.37 log cds/m2 (arrows in panel B) showing a depression of wave amplitudes in TG animals across all groups. (B) a-wave and b-wave amplitude as a function of stimulus strength. (C) a-wave and b-wave implicit time as a function of stimulus strength. n=9-19. **p<0.001.

**11**

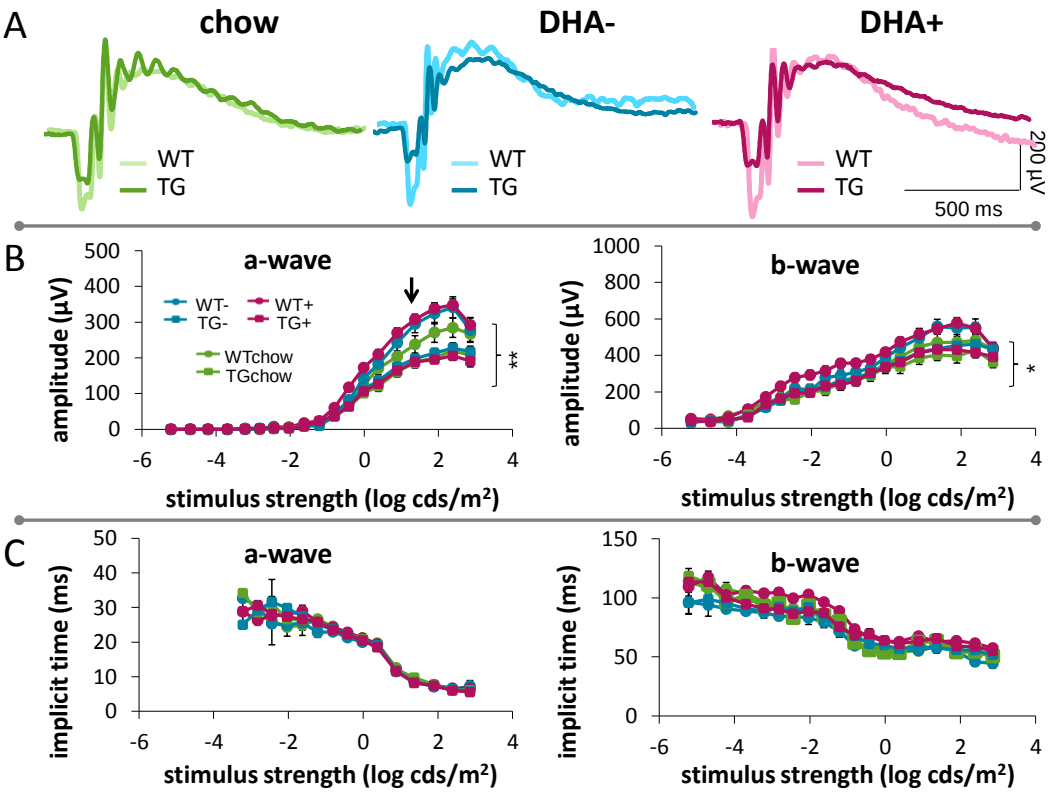


***Figure 11.*** **Scotopic intensity response at 3 months.** (A) Representative ERG traces at a stimulus intensity of 1.37 log cds/m$^2$ (arrow in panel B). Wave amplitudes are depressed for TG animals on chow and DHA- diets, while DHA+ shows preserved b-wave amplitudes. (B) a-wave and b-wave amplitude as a function of stimulus strength. (C) a-wave and b-wave implicit time as a function of stimulus strength. n=9-18. **p<0.001, *p<0.05.

### *4.1B) Photopic Intensity Response (PIR)*

Minimal changes were observed in cone-dependent vision over time (Figures 12 and 13). By 3 months, there was less variability among the 6 experimental groups and only slight decreases in a- and b-wave amplitudes were observed compared with ERG recordings from 1 month. Implicit time displayed no significant differences.

Similarly, genetic and dietary manipulations had no significant impact on a- and b-wave parameters (Figures 12B and 13B). A-wave amplitudes among all 6 experimental groups were variable and no patterns regarding effects of genotype or diet were detected. Conversely, b-wave amplitudes and a- and b-wave implicit times for all groups displayed similar responses (Figures 12C and 13C). There was little variability in these parameters.

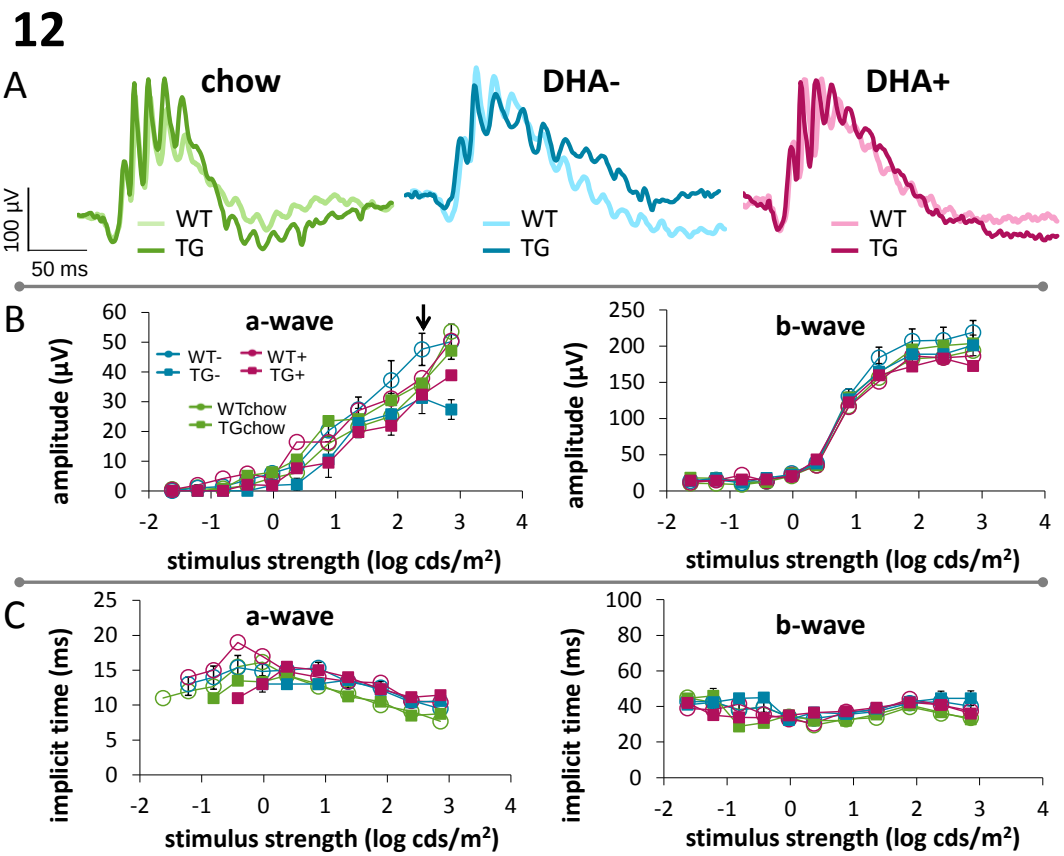


***Figure 12.*** **Photopic intensity response at 1 month.** (A) Representative ERG traces at a stimulus intensity of 2.86 log cds/m$^2$ (arrow in panel B). b-wave parameters are consistent throughout all groups, but a-wave amplitudes are varied. TG amplitudes are typically smaller with the exception of chow fed mice. (B) a-wave and b-wave amplitude as a function of stimulus strength. (C) a-wave and b-wave implicit time as a function of stimulus strength. n=9-19.

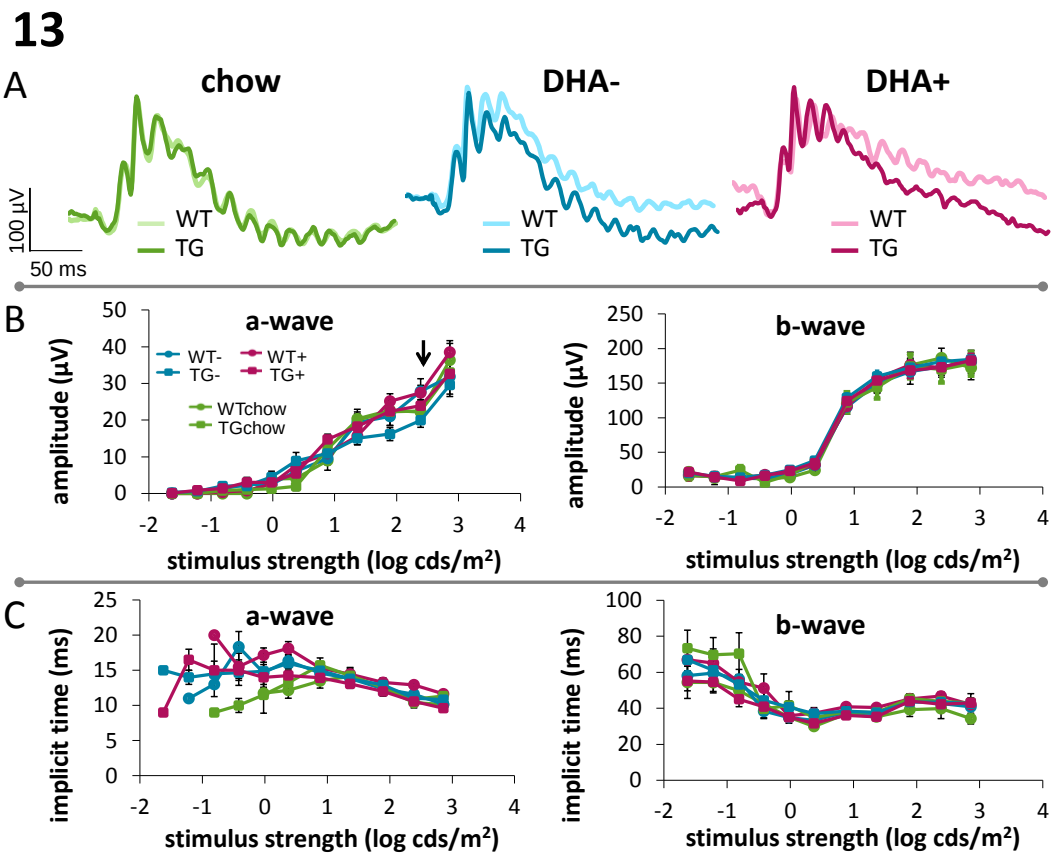


***Figure 13.*** **Photopic intensity response at 3 months.** (A) Representative ERG traces at a stimulus intensity of 2.86 log cds/m$^2$ (arrow in panel B) showing little differences in wave onset and amplitude across all groups. (B) a-wave and b-wave amplitude as a function of stimulus strength. (C) a-wave and b-wave implicit time as a function of stimulus strength. n=9-18.

**4.2) Anatomy**

Coinciding with previous findings (Kuny et al, 2012), photoreceptor numbers were significantly reduced across all eccentricities of the retina in TG compared to WT mice regardless of diet (Figure 14). Results also illustrated a gradient effect on photoreceptor death, with the center being the most severe and the periphery the least affected. Photoreceptor loss in the center, middle, and periphery was at about 36%, 27%, and 20%, respectively, when comparing TG to WT. Antenatal dietary manipulations, on the other hand, had no effect on photoreceptor counts.

**14**

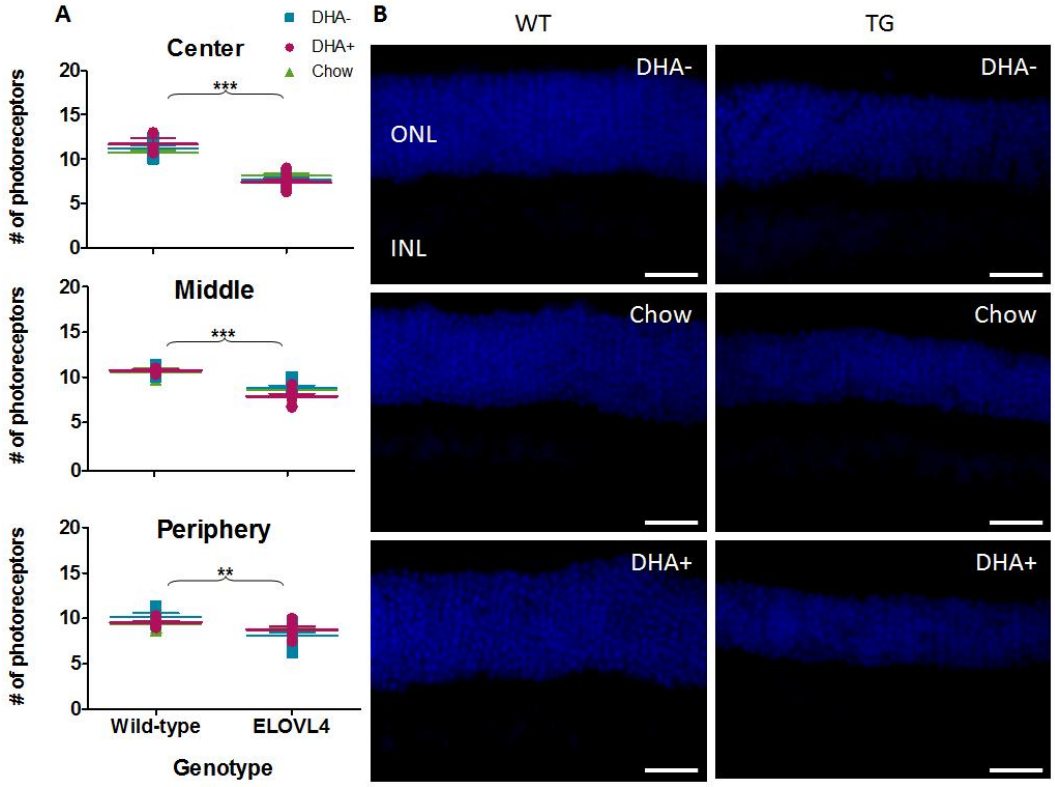


***Figure 14.*** **Comparison of photoreceptor numbers at 3 months.** (A) Photoreceptor loss at all eccentricities of the retina is apparent in transgenic animals. (B) Representative images from the central retina depicting photoreceptor loss in transgenic animals (blue, DAPI- stained cell bodies). Scale bar, 25 µm. ONL, outer nuclear layer; INL, inner nuclear layer. n= 4-8. ** $p<0.005$ and *** $p< 0.001$.

### 4.3) Retinal Fatty Acid Profile

Figure 15A illustrates that the level of DHA in TG neural retinas was significantly decreased by 35% in comparison to their WT littermates ($p<0.001$). On the other hand, the level of AA remained stable between the genotypes. This decline in DHA and stability of AA contributed to an overall significant decrease in DHA/AA ratio for the TG animals compared to WT ($p<0.001$). Results also indicated the high variability of the ELOVL4 TG genotype compared to WT in regards to fatty acid lipid profile (Figure 15B).

For WT animals supplemented with DHA (Figure 15B, left column), it is apparent that there was no difference in DHA levels compared to those not supplemented with DHA, rejecting the hypothesis that DHA supplementation would result in elevated retinal DHA levels compared to non-supplemented animals. Interestingly, the level of AA was significantly reduced ($p<0.05$). This resulted in an overall rise in DHA/AA level ratios ($p<0.05$). Referring to TG animals (Figure 15B, right column), alternatively, we observed declines both in DHA ($p<0.05$) and AA levels ($p<0.005$) for those supplemented with DHA compared with those non-supplemented. It is of no surprise to observe reduced levels of retinal AA in these animals; however it is peculiar that DHA levels should fall below that of their non-supplemented counterparts. Conversely, when evaluating the ratio of DHA/AA ratios between these animals, no differences were found.

15

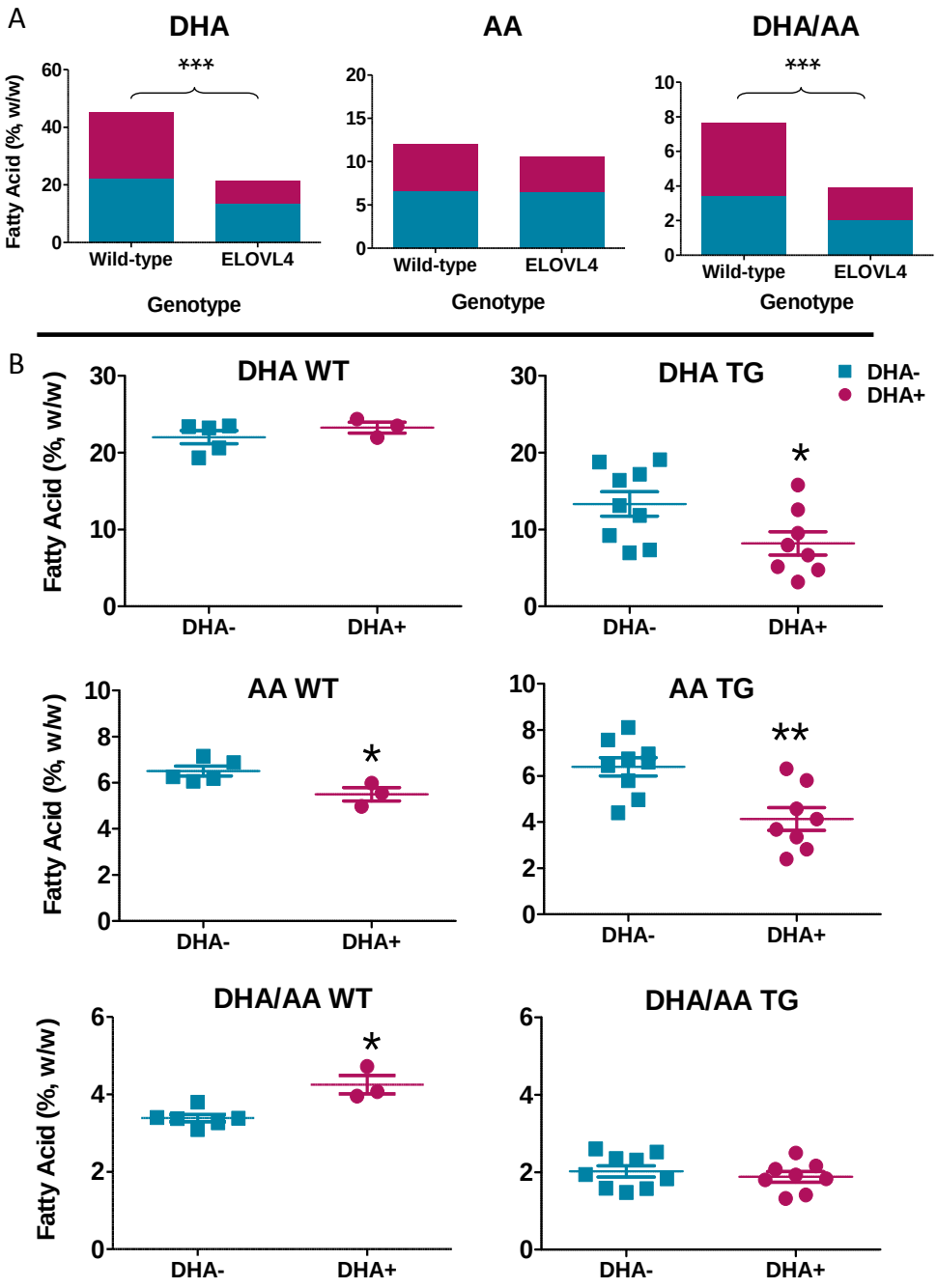


***Figure 15.*** **Retinal DHA and AA levels at 3 months.** (A) DHA and DHA/AA ratio levels were decreased in TG retinas. (B) Reduced retinal AA and augmented DHA/AA ratio levels in DHA fed WT mice. Interestingly, DHA supplementation resulted in decreased DHA and AA levels in TG retina. n=3-9. *p<0.05, **p<0.005, and ***p< 0.0001

# Chapter 5. DISCUSSION

## 5.1) Effect on Function

### *5.1A) Scotopic Intensity Response*

Comparisons between dark-adapted responses of 1 and 3 month old mice (regardless of genotype or diet) reveal an age-related functional decline involving decreased a- and b-wave amplitudes and increased implicit times. Several factors can contribute to functional disturbances over time such as programmed cell death, photo-oxidative damage of photoreceptors, and growth of the eye. Of these possibilities, eye growth is most likely to account for age-related functional change. Although loss of retinal nerve cells will cause diminished ERG a-and b-wave amplitudes, the events leading up to cell death, either by naturally occurring cell death or photo-oxidation, are unlikely to have considerable contributions. Studies on mice retinal development suggest that between postnatal day 15 and 20, both cellular division and naturally occurring cell death of all retinal cells have ceased (Finlay, 2008; Sharma et al, 2003; Mervin & Stone, 2002; Mu et al, 2001). Apoptosis of retinal nerve cells, therefore, that might occur between 1 month (postnatal day 30) and 3 months of age are essentially negligible. Several studies have also shown the harmful effects of bright light exposure on retina function (Thomas et al, 2012; Hunter et al, 2012), therefore high intensity flashes presented in SIR and PIR ERG recordings should be evaluated. At 2.86 log $cd \cdot s/m^2$, the final step of SIR ERG is considered too bright for human participants to endure. However, considering the limited time of exposure (10 μs) of these stimuli, the effects of light exposure and photo-oxidative damage would be

minimal. Okano et al (2012) and Maeda et al (2006) show that exposure of 12.5 log cd·s/$m^2$ for at least 30 min was required before 15% photoreceptor cell death was observed. More certainly, growth of the eye can account for the reduction in ERG response amplitudes. In a WT c57BL mouse, the eye will grow in axial length from about 3.05mm to 3.3mm between 1 and 3 months; an increase of almost 10% (Wisard et al, 2011). This growth, however, is unaccompanied by the expansion of the retina. Instead, components of the retina are stretched to match eye growth (Finlay, 2008). Smaller ERG wave amplitudes arise as the distance between the retina (ie. the source of light induced current modulation) and the corneal recording electrodes increases approximately 10%. A similar phenomenon occurs in the case of myopia and, in fact, the fully developed mouse eye has recently been considered myopic (Geng et al, 2011). Understanding the underlying mechanisms of age-dependent visual decline is important in its own entirety, but in context of retinal degeneration it can provide insight as to how it interacts with other factors involved in AMD pathology. We can assume that declines in visual responsiveness can occur naturally with age and without the influence of genetics and diet.

This does not imply that there is no genotype influence. ERG data also indicated a significant decline in a- and b-wave amplitudes in TG compared to WT groups in dark-adapted conditions. A more prominent and earlier effect of genotype on scotopic a-wave amplitude responses might suggest rod photoreceptor vulnerability in comparison to bipolar cells. Because implicit time was not influenced by genotype, it is also assumed that biochemical integrity is

intact. So, what makes rod photoreceptors susceptible to the *ELOVL4* genetic mutation? A major defect in this mutation is the inability of the encoded protein to elongate very long chain polyunsaturated fatty acids (VLC-PUFA) that may be highly involved in rod photoreceptor structure and activity. VLC-PUFAs primarily reside in rod outer segments, where their biophysical properties offer the ideal lipid membrane fluidity to modulate ion channel and enzyme activity (Agbaga et al, 2010). Several others have also indicated the particular interaction that these FA have with rhodopsin, providing structural stability and influencing its conformational state (Soubias & Gawrisch, 2006; Li et al, 2004; Aveldano 1988). Finally, Agbaga et al (2010) suggest that VLC-PUFA, as a constituent of the lipid membrane bilayer, cooperate with the RPE during outer segment shedding. Unable the generate VLC-PUFA; the *ELOVL4* mutation compromises a major structural and functional component of rod outer segments, ultimately leaving the rod system in a more vulnerable state than bipolar cells. On the other hand, the intimate interactions between the RPE and photoreceptor cells (rods in particular) also have the potential to interfere with the viability of these cells. In this TG mouse model, numerous reports of lipofuscin accumulation within the RPE have been made (Kuny et al, 2012; Vasireddy et al, 2010; Vasireddy et al, 2009). An unhealthy RPE can directly affect the quantity and quality of oxygen and nutrients being supplied to the cells they intimately interact with, causing them to deteriorate. Therefore, both the lack of VLC-PUFA and the interaction with unhealthy RPE can contribute to the vulnerability of the photoreceptor cells compared to bipolar cells of TG animals.

Diet, alternatively, does not appear to have an effect on retinal responsiveness at 1 month, but by 3 months it is obvious that chow diet is deleterious for WT mice. This is true for both a-and b- wave amplitude. However, it is difficult to make a direct comparison between the standard laboratory diet and fresh, custom prepared diets. Any disparity in food composition, preparation, or storage can contribute to the difference observed between the chow diet and the DHA+/- diets. Therefore, the deleterious effects of the chow diet are more likely to reflect the nature of the diet than its percentage of DHA content. Finally, to address the effects of diet on retinal function, it does not appear that antenatal DHA supplementation maintains retinal responsiveness in TG animals in the context of scotopic conditions. This opposes our prediction. It was thought that DHA accretion in the retina would, in some way, preserve retinal function by interacting with VLCFA metabolism or contributing to photoreceptor structural integrity. Based on ERG data alone, it can be interpreted that cell numbers and biochemical mechanisms of the retina are similar between these groups of animals. There are a couple of possible explanations for why beneficial effects of DHA were not achieved in this study. Although, 2% w/w DHA of total fatty acid has been shown to elicit a positive effect in rodent models (Suh et al, 1994), it is possible that this amount was insufficient to raise retinal DHA levels and elicit subsequent significant changes in function and anatomy for this specific animal model. Other studies have employed upwards of 5-9% w/w DHA of total fatty acid before noting significant changes in retinal DHA levels (Schnebelen et al, 2009; Yoshizawa & Tsubura, 2005; Nishizawa et al, 2003). To fully appreciate

the effects of DHA in this animal model of STGD3, future research can include increasing the percentage of DHA in the diet or providing an incremental amount of DHA to observe its effects on function in a dose dependent manner. An alternative explanation for the inefficiency of DHA to maintain retinal responsiveness may be related to antenatal dietary supplementation. By feeding parents the respective diet upon breeding, we make the assumption that the percent of DHA accumulated in the mothers' system is the same among all mothers on the day of conception. The diet that we are providing dams may, in actuality, not be indicative of the percentage of DHA that pups are receiving during critical developmental periods.

All in all, scotopic ERG responses revealed that eye growth is the most likely cause for diminished wave amplitudes over time, that rod photoreceptors are especially vulnerable to the effects of the mutated gene, and that 2% DHA antenatal supplementation was ineffective in maintaining scotopic retinal responses.

### *5.1B) Photopic Intensity Response*

Light-adapted responses were variable and generated no detectable patterns at either time point. It should also be clarified that responses to photopic light stimulation are less defined than scotopic conditions, making it more difficult to analyze and likely causing the variability displayed in wave amplitudes. Taking this into account, photopic responses still indicate no effect of age, genotype, or diet on wave amplitudes and implicit time under photopic

conditions, implying the stability of cone-driven vision. The rod system, therefore, is assumed to be the primary and main defect in STGD3 pathology and to also be more sensitive to the effects of diet.

Although changes in photopic responses due to the *ELOVL4* mutation are not evident at these early stages, it does not preclude them from occurring later on. Kuny et al (2012) have noted changes in cone photoreceptor numbers do not occur until 18 months of age in the same TG animal model. In any case, many cases of retinal degeneration, rod photoreceptor death precedes that of cones. It is not fully understood why cone degeneration occurs after rod death, but several reasons have been suggested. Studies have shown that diffusible factors, rod-derived cone viability factor for instance, released by healthy rod photoreceptors are critical for cone survival (Leveillard et al, 2004; Streichert et al, 1999; Mohand-Said et al, 1998). The collapse of rod ONL and consequent rod death often results in the creation of reactive oxygen species and a nutrient deprived environment, putting additional strain on the viability of cone photoreceptors (Montana et al, 2012; Komeima et al, 2006). These discoveries further enhance the need to study early changes in retinal degeneration in pursuit to prevent subsequent deterioration of high-acuity vision.

As with SIR, photopic responses were unaffected by dietary DHA manipulation. This is no surprise for it is evident that the cone system is more resistant to perturbations than rods are regarding this form of retinal degeneration.

### 5.2) Effect on Photoreceptor Numbers

With the *ELOVL4* mutation, 3-month-old mice had diminished photoreceptor cell numbers compared to WT. This was true across all eccentricities of the retina, affecting the center and middle more than the periphery. The same phenomenon is described in animal models (Kuny et al, 2012; Karan et al, 2005) and human STDG3 and macular degeneration (Ramkumar et al, 2010; Gao & Hollyfield, 1992), verifying that this model of retinal degeneration is a relatively reliable research tool. Photoreceptor death in TG retinas coincides with functional differences observed between these animals and WT animals in scotopic ERG at 3 months of age, offering an explanation for why the difference in a-wave amplitudes between these genotypes at 3 months are greater in comparison to 1 month differences (Figures 10 and 11). Coincidently, the functional decline in TG animals compared to WT animals is at about 37% at 3 months; comparable to the photoreceptor loss observed at the center of the retina (36%). These findings are also in agreement with a report from Kuny et al (2012) that demonstrates that rod photoreceptor death does not occur until 2 months of age. In summary, the *ELOVL4* mutation in this mouse model replicates retinal degeneration observed in humans, affecting rod photoreceptors predominantly in the center.

Rejecting our hypothesis, antenatal dietary supplementation was ineffective in preserving photoreceptor numbers in this study. It was believed that DHA supplementation would offer structural support for photoreceptor outer segments. As outlined by SanGiovanni and Chew (2005), DHA acts a major

structural lipid to maintain photoreceptor permeability, fluidity, and thickness. All these properties are vital for not only maintaining structural integrity, but for phototransduction as well. Results from this study do not necessarily imply that DHA is unable to preserve the properties responsible for maintaining photoreceptor integrity. Again, it is possible that 2% DHA over total FA supplied antenatally was not enough to elicit changes. Perhaps if we increased the amount of DHA being supplied to the mice, we might observe a larger accretion in retinal tissue and consequent preservation of retinal integrity.

**5.3) Effect on Lipid Profile**

The effects of genotype and antenatal dietary supplementation on retinal fatty acids yielded intriguing results. In TG retinas, a significant decrease in DHA levels contributed to an overall decrease in DHA/AA levels compared to their WT counterparts. Considering the loss of DHA-containing outer segments in photoreceptors of TG animals, the decline of DHA in their retinas can be accounted for. Moreover, because the levels of AA in photoreceptor cells are negligible (SanGiovanni & Chew, 2004), it is reasonable that retinal AA levels were stable between TG and WT animals. Reduced retinal DHA level is often observed in both animal and human subjects in the context of retinal degeneration.

In contrast to previously described outcome measures in this study, DHA supplementation produced an effect on retinal DHA and AA levels. Referring first to WT retinas, it was interesting to see that although mice were fed with DHA antenatally, their DHA levels were not increased in comparison to those non-

supplemented. AA, conversely, was significantly reduced which resulted in an overall higher DHA/AA ratio level for the DHA supplemented versus the DHA deprived. Aguirre et al (1997) have reported similar findings. By providing DHA-enriched supplements in progressive rod-cone degeneration affected dogs, they managed to elevate plasma and liver DHA; however, retinal DHA levels remained constant. They proposed that an upper limit of DHA content in rod outer segments was reached, thereby reducing the incorporation of DHA from RPE cells to photoreceptors. Despite being unable to increase retinal DHA levels, it is evident that this quantity of DHA was sufficient to lower AA levels, perhaps by introducing an imbalance of omega-3 to 6 ratio and directing competing enzymes to favour the omega-3 FA metabolic pathway.

Yielding different results in TG animals, it appears there is an interaction between genotype and DHA supplementation. In the context of the TG mutation, DHA supplementation managed to decrease both retinal DHA and AA levels in comparison to non-supplementation (DHA- diet). The reduction of these FA, however, matched the proportions of DHA and AA in non-supplemented animals, so no significant difference was found in DHA/AA ratios between these experimental groups. A notable confound in these results is the decrease of retinal DHA in supplemented animals beyond even the level of DHA in deprived animals. Following the previous assumption that external introduction of DHA would cause an imbalance of omega-3 and -6 FA metabolism in favour of omega-3, it is logical that retinal AA levels are significantly reduced in DHA fed animals. Still, this cannot fully explain why retinal DHA levels are depressed. Rather, it

would suggest that omega-3 FA (ie. DHA) should be increased. One postulation is that 1) the inability of the mutated ELOVL4 protein to elongate VLCFA and 2) the favorability towards the omega-3 FA metabolic pathway causes an accumulation of downstream omega-3 FA substrates. This accumulation, in turn, potentially activates a negative feedback mechanism that prevents further elongation of omega-3 FA. This regulatory system has also been previously suggested by Terre'Blanche et al (2011). They proposed that elevated DHA levels would "exert a negative feedback mechanism on the elongase enzyme responsible for the elongation of EPA (C20:5(3)) to DPA (C22:5(3))." If this is true, it would still only answer part of the problem. We want to understand not just why retinal DHA levels were not elevated in DHA supplemented TG animals, but why they fell below non-supplemented animals. Perhaps, RPE cells were also able to detect the accumulation of downstream omega-3 substrates and, in response, limit the incorporation of DHA into rod photoreceptors. Under normal conditions, RPE delivers recycled DHA from shed outer segment disc membranes to the inner segments of photoreceptors (Bazan, 2009). This pathway, describing the RPE's role in incorporating DHA into photoreceptors, is known as the "short loop." Based on the results from the current study, it can be proposed that the short loop is restrained to due excessive omega-3 FA levels. Both mechanisms of negative feedback and limited DHA incorporation would explain the significant decline of DHA in retinal tissue, especially in an animal model with defective ELOVL4 enzymes. However, these proposed mechanisms should be taken with a grain of salt as they are only conjectures. To summarize and to address the hypothesis,

antenatal DHA supplementation did not prevent decline of retinal DHA in TG animals and DHA levels in WT retinas were comparable.

### 5.4) Summary

The animal model employed in this study represents a reliable tool to study retinal degeneration. Though no animal model can perfectly replicate disease symptoms observed in human pathology, a similarity in major phenotypes should be maintained in order to draw clinically applicable conclusions. We were able to show functional and anatomical changes in the retina of TG animals. Similar to humans, rod photoreceptor dysfunction preceded cones and photoreceptor loss was more prominent in the center than the periphery. Selecting an appropriate animal model augments the significance of findings and it relevance to clinical applications.

Unfortunately, antenatal DHA supplementation did not yield such positive outcomes. It had no significant effects on both function and anatomy, producing similar ERG responses and resulting in comparable photoreceptor numbers as non-supplemented mice. DHA supplementation demonstrated beneficial effects only in WT mice by lowering AA levels. Oddly, in TG retinas DHA levels were lower when supplemented with 2% DHA over total FA. Despite this, the overall retinal DHA/AA level remained akin to non-supplemented mice due to a proportional decline in AA levels. Everything considered, it does not seem that antenatal DHA dietary supplementation has a beneficial effect for TG animals.

### 5.5) Strengths and Limitations

What has been clear throughout this study is the consistency of the *ELOLV4* mouse model in displaying symptoms described in human Stargardt-like dystrophy. The selection of this animal model is validated by replicating diminished ERG responses, reduced photoreceptor cells, and lowered retinal DHA levels typically observed in human patients with retinal degeneration. The timeline for disease development in the TG1-2 line of this *ELOVL4* mouse is also appropriate, providing enough time to observe the gradual progression of retinal degeneration. Concurrently, the disease progression is quick enough to observe functional changes at 1 month. This study was the first report functional changes at this early time point, therefore, corroborating the use of electroretinography as a sensitive equipment to measure retinal function. Despite employing the ERG at 1 month in the same mouse model, previous research in our lab was unable to detect the same changes from the current study (unpublished results). By increasing the number of animals used in this study (n=70) and eliminating inter-observer variability (data analyzed by only 1 person), the reliability of this study is optimized. Additionally, data were evaluated under blind conditions, revealing the genotype of the animals only after analysis was performed. This project is not perfect, but does contain elements that warrant it to be reliable.

Several limitations arose in this study. First, the duration that dams received custom, prepared diets before conception of their pups were variable among all breeder pairs, potentially allowing more time for some mothers to accumulate systemic DHA levels. To control for this in the future, it would be

recommended that parents be maintained on respective diets for at least 1 week (or until blood plasma levels or DHA are similar within groups) before breeders are matched. This would ensure that pups are receiving the desired proportion of DHA from their mothers. Furthermore, it was found that standard laboratory chow was not the ideal baseline control diet. The overall composition of the diet differs considerably from the custom made diets. In hindsight, it would have been wiser to prepare a homemade diet containing DHA levels equivalent to the amount offered in the standard laboratory chow. Finally, it became evident that preparing and counting photoreceptor cells introduces variability and subjectivity. Before reaching the final step of counting photoreceptors cells, a long process of preparing retinal cross sections must be performed. Variability in extracting and embedding tissue could lead to variability in the integrity and the cutting angle of retinal cross-sections, respectively. These inconsistencies can then contribute to difficulties in selecting representative, yet intact tissue for photoreceptor cell counting. The system of counting cells is also highly subjective. Altogether, the methodology of preparing retinal cross sections and counting photoreceptor cells is not the most reliable measure. For a more complete picture, western blots using photoreceptor specific markers, anti-rhodopsin antibody for example, should be used in conjunction with anatomical assessment. Though this study was not void of weaknesses, these limitations can be easily adjusted in the future.

### 5.6) Future Directions

The findings from the current study provide only part of a complete picture. To further develop our understanding of how dietary DHA supplementation affects the disease progression inherent with the *ELOVL4* mutation, we can perform various other outcome measures. First, we can study the effects of genotype and diet interaction on tissues other than the retina. Although the expression of the mutated gene is under the direction of the IRBP promoter found between the photoreceptors and RPE, the retina is not completely isolated but has many interactions with other body systems. The liver, for example, is responsible for delivering systemic DHA to the RPE. Bazan (2009) describes this pathway as the "long loop." Dietary omega-3 FA acids (e.g., ALA, EPA, or DHA) undergo a series of elongations and desaturations in the liver before being tagged with phospholipids and transported systemically as phospholipids to the RPE (or brain and to a smaller extent, the testis). As previously described, the RPE is involved in the "short loop," incorporating DHA from the extracellular matrix to photoreceptor cells (Bazan, 2009). All these systemic interactions justify the requirement to collect blood, liver, and RPE tissue to determine alternative storage of DHA. Awareness of how DHA is distributed could also help explain why DHA supplementation was capable of lowering retinal DHA levels of TG animals in this study. Could the long or short loop be somehow compromised?

As a method to study the effects of the *ELOVL4* transgene, measures of a vitamin A derived pyridinium bisretinoid (A2E), a constituent of toxic lipofuscin, have been conducted to determine the progression of retinal degeneration. Studies

have reported this accumulation in STGD3 animal models (Kuny et al, 2012) and reduced levels upon DHA supplementation (Dornstauder et al, 2012). To further enhance our knowledge of how extracellular deposits can be altered by introducing DHA, we can use optical coherence tomography (OCT) and fundus photography in parallel with A2E measures. OCT and fundus images are valuable research tools in that they can provide an anatomical account for the localization of extracellular debris deposition. This could aid us in identifying vulnerable regions of the retina from both a cross-sectional (OCT imaging) and fundoscopic point of view. An added benefit is that these are non-terminal measures that would allow for observation of disease progression within the same animals.

Results from this study also have implications that 2% w/w DHA of total fatty acid content supplied antenatally does not necessarily maintain or preserve retinal responsiveness and structure. It would be worthwhile, therefore, to explore different concentrations of DHA in the diet, studying its effect in a dose dependant manner. An alternative method is to alter the concentration of omega-3 to -6 in the diet to investigate the optimal ratio required to sustain retinal function and integrity. Simon et al (2011) used a similar approach to monitor levels of retinal omega-3 fatty acid incorporation and gene expression modification. Here, they demonstrated providing high levels of DHA and low levels of LA in parallel yielded the optimal results. Yet another study suggests a combination of omega-3 and -6 FA in the diet is more effective for eye health than single supplementation (Schnebelen et al, 2009). In a similar vein, we may discover that developing a balance between omega-3 and -6 levels is more beneficial than simply raising

DHA levels. However, this will remain uncertain until dietary manipulations in this animal model of retinal degeneration are implemented.

One month changes discovered in this study warrants examination of early mechanisms involved in retinal dysfunction as well. This is a critical time period, for it signifies that by 1 month the retina is unable to tolerate and counteract the negative effects of the genetic mutation anymore, leading to the presentation of the disease phenotype. It would be worthwhile, hence, to focus on the mechanisms contributing to this functional disturbance, whether anatomical or molecular, at this time point. A decline in a-wave amplitude could imply photoreceptor death, however markers for apoptosis (TUNEL), UPR (Kuny et al, 2012), and oxidative stress (unpublished) have all been examined at this time point but were not detected in TG mice. In the same study, FGF2 in photoreceptors and GFAP in Müller cells were found to be upregulated at one month. Though both are indicators of distress, it is difficult to identify the cause leading up to their over-expression. For future research, we could examine the molecular contents of photoreceptor cells. Could alterations in FA content within outer segment membranes disrupt the structure and functioning of ion channels and proteins involved in dark current? After all, it has previously been emphasized the vital role VLCUFA has on the dynamics involved with phototransduction (Soubias & Gawrisch, 2005; Li et al, 2004; Aveldano 1988).

Finally, it is still not fully understood why retinal DHA levels are reduced in DHA fed TG animals. It was proposed that feedback mechanisms and dampening of the omega-3 fatty acid metabolic pathway could account for

diminished DHA levels in the retina. To expand our comprehension of how dietary DHA supplementation interacts with the *ELOVL4* mutation, it would be worthwhile to assess the activity of the elongases, desaturases, and any other possible enzymes that may be involved in the metabolic pathway. Most other studies have measured fatty acid ratios (e.g. DHA/EPA) as method to evaluate the activity of elongases and desaturases along the fatty acid metabolic pathway (Terre/Blanche et al, 2011; Martinez et al, 2010), however it would be more comprehensive if it is possible to monitor down (or up) regulation of these protein using specific markers in conjunction. Additionally, oxidative stress levels could be monitored. Although unpublished data reveal that oxidative stress is undetected in the TG model, but it is possible that the introduction of highly oxidizable DHA could induce oxidative stress (Tanito et al, 2008). Suh et al (2009) demonstrated that elevated levels of omega-3 FA, including DHA, in their Fat-1 mouse model produced increased levels of GFAP and carboxyethylpyrrole (CEP, a protein adduct generated from DHA oxidation) in Muller cells and photoreceptors, respectively. An increase, therefore, in CEP in the context of DHA supplementation in the *ELOVL4* TG model could indicate the oxidation (and explain the decline) of DHA.

The results from the current study offer a great start in understanding the pathology underlying retinal degeneration and its interaction with DHA supplementation; however, several more procedures can be implemented to widen the scope of our knowledge in this field.

## 5.7) Conclusions

Before DHA can be recommended or rejected, more research should be conducted to study the pathology of the *ELOVL4* mutation. Results from this study direct our focus towards rod photoreceptor outer segments. Here, both DHA and VLCPUFA are found in high quantities (Agbaga et al, 2012) and have been suggested to be integral structural and functional components (Soubias et al, 2005; Aveldano 1988). The intricate interaction between VLC-PUFA in lipid membranes and the RPE during outer segment shedding, if compromised, would affect the recycling and incorporation DHA back into rod photoreceptors. With so many unsolved mysteries regarding STGD3 pathology and omega-3 fatty acid metabolism, it is difficult to completely comprehend how DHA dietary supplementation interacts with the *ELOVL4* mutation. Based on our findings, DHA has neither a therapeutic or harmful effect on retinal degeneration.

**Literature Cited**

Agbaga, M., Brush, R. S., Mandal, M. N. A., Henry, K., Elliott, M. H., & Anderson, R. E. (2008). Role of stargardt-3 macular dystrophy protein (ELOVL4) in the biosynthesis of very long chain fatty acids. *Proceedings of the National Academy of Sciences, 105*(35), 12843-12848. doi:10.1073/pnas.0802607105

Agbaga, M., Mandal, M. N. A., & Anderson, R. E. (2010). Retinal very long-chain PUFAs: New insights from studies on ELOVL4 protein. *Journal of Lipid Research, 51*(7), 1624-1642. doi:10.1194/jlr.R005025

Anderson, R. E., Maude, M. B., & Bok, D. (2001). Low docosahexaenoic acid levels in rod outer segment membranes of mice with rds/Peripherin and P216L peripherin mutations. *Investigative Ophthalmology & Visual Science, 42*(8), 1715-1720.

Augood, C., Chakravarthy, U., Young, I., Vioque, J., de Jong, P. T., Bentham, G., et al. (August 2008). Oily fish consumption, dietary docosahexaenoic acid and eicosapentaenoic acid intakes, and associations with neovascular age-related macular degeneration. *The American Journal of Clinical Nutrition, 88*(2), 398-406.

Aveldano, M. I. (1988). Phospholipid species containing long and very long polygenic fatty acids remain with rhodopsin after hexane extraction of photoreceptor membranes. *Biochemistry, 27*(4), 1229-39.

Bazan, N. G. (2009). Cellular and molecular events mediated by docosahexaenoic acid-derived neuroprotectin D1 signalling in photoreceptor cell survival and brain protection. *Prostaglandins, Leukotrienes and Essential Fatty Acids, 81*(2–3), 205-211. doi:10.1016/j.plefa.2009.05.024

Bazan, N. G., Molina, M. F., & Gordon, W. C. (2011). Docosahexaenoic acid signalolipidomics in nutrition: Significance in aging, neuroinflammation, macular degeneration, Alzheimer's, and other neurodegenerative diseases. *Annual Review of Nutrition, 31*(1), 321-351. doi:10.1146/annurev.nutr.012809.104635

Bhutto, I., & Lutty, G. (2012). Understanding age-related macular degeneration (AMD): Relationships between the photoreceptor/retinal pigment epithelium/Bruch's membrane/choriocapillaris complex. *Molecular Aspects of Medicine, 33*(4), 295-317. doi:10.1016/j.mam.2012.04.005

Bird, A. C. (2010). Therapeutic targets in age-related macular disease. *The Journal of Clinical Investigation, 120*(9), 3033-3041. doi:10.1172/JCI42437

Breslow, J. L. (2006). n−3 fatty acids and cardiovascular disease. *The American Journal of Clinical Nutrition, 83*(6), S1477-1482S.

Calandria, J., & Bazan, N. (2010). Neuroprotectin D1 modulates the induction of pro-inflammatory signalling and promotes retinal pigment epithelial cell survival during oxidative stress. In R. E. Anderson, J. G. Hollyfield & M.

M. LaVail (Eds.), (pp. 663-670) Springer New York. doi:10.1007/978-1-4419-1399-9_76

Cameron, D. J., Tong, Z., Yang, Z., Kaminoh, J., Kamiyah, S., Chen, H., et al. (2007). Essential role of Elovl4 in very long chain fatty acid synthesis, skin permeability barrier function, and neonatal survival. *International Journal of Biological Sciences, 3*(2), 111-119.

Cheung, L. K., & Eaton, A. (2013). Age-related macular degeneration. *Pharmacotherapy: The Journal of Human Pharmacology and Drug Therapy,* doi:10.1002/phar.1264

Chiu, C., Klein, R., Milton, R. C., Gensler, G., & Taylor, A. (2009). Does eating particular diets alter the risk of age-related macular degeneration in users of the age-related eye disease study supplements? *British Journal of Ophthalmology, 93*(9), 1241-1246. doi:10.1136/bjo.2008.143412

Ciulla, T. A., & Rosenfeld, P. J. (2009). Antivascular endothelial growth factor therapy for neovascular age-related macular degeneration. *Current Opinion in Ophthalmology, 20*(3), 158-165.

Damico, F. M., Gasparin, F., Scolari, M. R., Pedral, L. S., & Takahashi, B. S. (2012). New approaches and potential treatments for dry age-related macular degeneration. *Arquivos Brasileiros De Oftalmologia, 75*(1), 71-76.

Delcourt, C. (2007). Application of nutrigenomics in eye health. *Nutrigenomics - Opportunities in Asia, 60,* 168-175.

Ding, X., Patel, M., & Chan, C. (2009). Molecular pathology of age-related macular degeneration. *Progress in Retinal and Eye Research, 28*(1), 1-18. doi:10.1016/j.preteyeres.2008.10.001

Donoso, L. A., Edwards, A. O., Frost, A., Vrabec, T., Stone, E. M., Hageman, G. S., et al. (2001). Autosomal dominant Stargardt-like macular dystrophy. *Survey of Ophthalmology, 46*(2), 149-163. doi:10.1016/S0039-6257(01)00251-X

Dornstauder, B., Suh, M., Kuny, S., Gaillard, F., MacDonald, I. M., Clandinin, M. T., et al. (2012). Dietary docosahexaenoic acid supplementation prevents age-related functional losses and A2E accumulation in the retina. *Investigative Ophthalmology & Visual Science, 53*(4), 2256-2265. doi:10.1167/iovs.11-8569

Evans Jennifer, R., & Lawrenson John, G. (2012). Antioxidant vitamin and mineral supplements for slowing the progression of age-related macular degeneration *John Wiley & Sons, Ltd.* doi:10.1002/14651858.CD000254.pub3

Finlay, B. L. (2008). The developing and evolving retina: Using time to organize form. *Brain Research, 1192*(0), 5-16. doi:10.1016/j.brainres.2007.07.005

Gao, H., & Hollyfield, J. G. (1992). Aging of the human retina. differential loss of neurons and retinal pigment epithelial cells. *Investigative Ophthalmology & Visual Science, 33*(1), 1-17.

Gehrs, K. M., Anderson, D. H., Johnson, L. V., & Hageman, G. S. (2006). Age - related macular degeneration—emerging pathogenetic and therapeutic concepts. *Annals of Medicine, 38*(7), 450-471. doi:10.1080/07853890600946724

Geng, Y., Schery, L. A., Sharma, R., Dubra, A., Ahmad, K., Libby, R. T., et al. (2011). Optical properties of the mouse eye. *Biomedical Optics Express, 2*(4), 717-38.

Grayson, C., & Molday, R. S. (2005). Dominant negative mechanism underlies autosomal dominant stargardt-like macular dystrophy linked to mutations in ELOVL4. *Journal of Biological Chemistry, 280*(37), 32521-32530. doi:10.1074/jbc.M503411200

Hartveit, E. (1999). Reciprocal synaptic interactions between rod bipolar cells and amacrine cells in the rat retina. *Journal of Neurophysiology, 81*(6), 2923-2936.

Henkind P, Hansen RI, Szalay J. Ocular circulation. In: Records RE, editor. Physiology of the human eye and visual system. *New York: Harper & Row*; 1979. p. 98-155.

Ho L, van Leeuwen R, Witteman JM, et al. (2011). Reducing the genetic risk of age-related macular degeneration with dietary antioxidants, zinc, and ω-3 fatty acids: The Rotterdam study. *Archives of Ophthalmology,* 129(6):758-766. doi:10.1001/archophthalmol.2011.141

Hooper, P., Jutai, J. W., Strong, G., & Russell-Minda, E. (2008). Age-related macular degeneration and low-vision rehabilitation: A systematic review. *Canadian Journal of Ophthalmology / Journal Canadien d'Ophtalmologie, 43*(2), 180-187. doi:10.3129/i08-001

Hubbard AF, Askew E, Singh N, Leppert M, Bernstein PS. (2006). Association of adipose and red blood cell lipids with severity of dominant Stargardt macular dystrophy (stgd3) secondary to an elovl4 mutation. *Archives of Ophthalmology,* 124(2):257-263. doi:10.1001/archopht.124.2.257

Hunter, J. J., Morgan, J. I. W., Merigan, W. H., Sliney, D. H., Sparrow, J. R., & Williams, D. R. (2012). The susceptibility of the retina to photochemical damage from visible light. *Progress in Retinal and Eye Research, 31*(1), 28-42. doi:10.1016/j.preteyeres.2011.11.001

Johnson, G. H., & Fritsche, K. (2012). Effect of dietary linoleic acid on markers of inflammation in healthy persons: A systematic review of randomized controlled trials. *Journal of the Academy of Nutrition and Dietetics, 112*(7), 1029-1041.e15. doi:10.1016/j.jand.2012.03.029

Kaarniranta, K., Salminen, A., Haapasalo, A., Soininen, H., & Hiltunen, M. (2011). Age-related macular degeneration (AMD): Alzheimer's disease in the eye? *Journal of Alzheimer's Disease, 24*(4), 615-631. doi:10.3233/JAD-2011-101908

Kanda, A., Abecasis, G., & Swaroop, A. (2008). Inflammation and the pathogenesis of age-related macular degeneration. *The British Journal of Ophthalmology, 92*, 448-450. doi:10.1136/bjo.2007.131581

Karan, G., Lillo, C., Yang, Z., Cameron, D. J., Locke, K. G., Zhao, Y., et al. (2005). Lipofuscin accumulation, abnormal electrophysiology, and photoreceptor degeneration in mutant ELOVL4 transgenic mice: A model for macular degeneration. *Proceedings of the National Academy of Sciences of the United States of America, 102*(11), 4164-4169. doi:10.1073/pnas.0407698102

Khandhadia, S., Cipriani, V., Yates, J. R. W., & Lotery, A. J. (2012). Age-related macular degeneration and the complement system. *Immunobiology, 217*(2), 127-146. doi:10.1016/j.imbio.2011.07.019

Khandhadia, S., Cipriani, V., Yates, J. R. W., & Lotery, A. J. (2012). Age-related macular degeneration and the complement system. *Immunobiology, 217*(2), 127-146. doi:10.1016/j.imbio.2011.07.019

Koch, C., Dölle, S., Metzger, M., Rasche, C., Jungclas, H., Rühl, R., et al. (2008). Docosahexaenoic acid (DHA) supplementation in atopic eczema: A

randomized, double-blind, controlled trial. . *British Journal of Dermatology, 158*, 786–792.

Kolb, H., & Famiglietti, E. V. (1974). Rod and cone pathways in the inner plexiform layer of cat retina. *Science, 186*(4158), 47-49.

Komeima, K., Rogers, B. S., Lu, L., & Campochiaro, P. A. (2006). Antioxidants reduce cone cell death in a model of retinitis pigmentosa. *Proceedings of the National Academy of Sciences, 103*(30), 11300-11305. doi:10.1073/pnas.0604056103

Krizaj, D. (2000). Mesopic state: Cellular mechanisms involved in pre- and post-synaptic mixing of rod and cone signals. *Microscopy Research and Technique, 50*(5), 347-359. doi:10.1002/1097-0029(20000901)50:5<347::AID-JEMT4>3.0.CO;2-D

Kuny, S., Gaillard, F., Mema, S. C., Freund, P. R., Zhang, K., MacDonald, I. M., et al. (2010). Inner retina remodeling in a mouse model of stargardt-like macular dystrophy (STGD3). *Investigative Ophthalmology & Visual Science, 51*(4), 2248-2262. doi:10.1167/iovs.09-4718

Leveillard, T., Mohand-Said, S., Lorentz, O., Hicks, D., Fintz, A., Clerin, E., et al. (2004). Identification and characterization of rod-derived cone viability factor. *Nature Genetics, 36*(7), 755-759.

Li, W., Chen, Y., Cameron, D. J., Wang, C., Karan, G., Yang, Z., et al. (2007). Elovl4 haploinsufficiency does not induce early onset retinal degeneration in mice. *Vision Research, 47*(5), 714-722. doi:10.1016/j.visres.2006.10.023

Litman, B., Niu, S., Polozova, A., & Mitchell, D. (2001). The role of docosahexaenoic acid containing phospholipids in modulating G protein-coupled signalling pathways. *Journal of Molecular Neuroscience, 16*(2-3), 237-242. doi:10.1385/JMN:16:2-3:237

Logan, S., Agbaga, M., Chan, M. D., Kabir, N., Mandal, N. A., Brush, R. S., et al. (2013). Deciphering mutant ELOVL4 activity in autosomal-dominant stargardt macular dystrophy. *Proceedings of the National Academy of Sciences, 110*(14), 5446-5451. doi:10.1073/pnas.1217251110

Luthert, P. J. (2011). Pathogenesis of age-related macular degeneration. *Diagnostic Histopathology, 17*(1), 10-16. doi:10.1016/j.mpdhp.2010.10.004

MacDonald, I. M., Hébert, M., Yau, R. J., Flynn, S., Jumpsen, J., Suh, M., et al. (2004). Effect of docosahexaenoic acid supplementation on retinal function in a patient with autosomal dominant stargardt-like retinal dystrophy. *British Journal of Ophthalmology, 88*(2), 305-306. doi:10.1136/bjo.2003.024299

Maeda, A., Maeda, T., Golczak, M., Imanishi, Y., Leahy, P., Kubota, R., et al. (2006). Effects of potent inhibitors of the retinoid cycle on visual function

and photoreceptor protection from light damage in mice. *Molecular Pharmacology, 70*(4), 1220-1229. doi:10.1124/mol.106.026823

Marmorstein, A. D., & Marmorstein, L. Y. (2007). The challenge of modeling macular degeneration in mice. *Trends in Genetics, 23*(5), 225-231. doi:10.1016/j.tig.2007.03.001

Martinez, M., Ichaso, N., Setien, F., Durany, N., Qiu, X., & Roesler, W. (2010). The Δ4-desaturation pathway for DHA biosynthesis is operative in the human species: Differences between normal controls and children with the zellweger syndrome. *Lipids in Health and Disease, 9*, 98.

McMahon, A., Butovich, I. A., Mata, N. L., Klein, M., Ill, R. R., Richardson, J., et al. (2007). Retinal pathology and skin barrier defect in mice carrying a stargardt disease-3 mutation in elongase of very long chain fatty acids-4. *Molecular Vision, 13*, 258-272.

Menger, N., & Wassle, H. (2000). Morphological and physiological properties of the A17 amacrine cell of the rat retina. *Visual Neuroscience, 17*(05), 769.

Mervin, K., & Stone, J. (2002). Regulation by oxygen of photoreceptor death in the developing and adult C57BL/6J mouse. *Experimental Eye Research, 75*(6), 715-722. doi:10.1006/exer.2002.2064

Michaelides, M., Hardcastle, A. J., Hunt, D. M., & Moore, A. T. (2006). Progressive cone and cone-rod dystrophies: Phenotypes and underlying

molecular genetic basis. *Survey of Ophthalmology*, *51*(3), 232-258. doi:10.1016/j.survophthal.2006.02.007

Mills, S. L., & Massey, S. C. (1999). AII amacrine cells limit scotopic acuity in central macaque retina: A confocal analysis of calretinin labeling. *The Journal of Comparative Neurology*, *411*(1), 19-34. doi:10.1002/(SICI)1096-9861(19990816)411:1<19::AID-CNE3>3.0.CO;2-4

Mohand-Said, S., Deudon-Combe, A., Hicks, D., Simonutti, M., Forster, V., Fintz, A., et al. (1998). Normal retina releases a diffusible factor stimulating cone survival in the retinal degeneration mouse. *Proceedings of the National Academy of Sciences*, *95*(14), 8357-8362.

Molday, R. S., & Zhang, K. (2010). Defective lipid transport and biosynthesis in recessive and dominant stargardt macular degeneration. *Progress in Lipid Research*, *49*(4), 476-492. doi:10.1016/j.plipres.2010.07.002

Molday, R. S., Zhong, M., & Quazi, F. (2009). The role of the photoreceptor ABC transporter ABCA4 in lipid transport and stargardt macular degeneration. *Biochimica Et Biophysica Acta (BBA) - Molecular and Cell Biology of Lipids*, *1791*(7), 573-583. doi:10.1016/j.bbalip.2009.02.004

Montana, C. L., Kolesnikov, A. V., Shen, S. Q., Myers, C. A., Kefalov, V. J., & Corbo, J. C. (2013). Reprogramming of adult rod photoreceptors prevents

retinal degeneration. *Proceedings of the National Academy of Sciences, 110*(5), 1732-1737. doi:10.1073/pnas.1214387110

Morse, N. L. (2012). Benefits of docosahexaenoic acid, folic acid, vitamin D and iodine on foetal and infant brain development and function following maternal supplementation during pregnancy and lactation. *Nutrients, 4*, 799-840.

Mu, X., Zhao, S., Pershad, R., Hsieh, T., Scarpa, A., Wang, S. W., et al. (2001). Gene expression in the developing mouse retina by EST sequencing and microarray analysis. *Nucleic Acids Research, 29*(24), 4983-4993. doi:10.1093/nar/29.24.4983

Nelson, R., & Kolb, H. (1985). A17: A broad-field amacrine cell in the rod system of the cat retina. *Journal of Neurophysiology, 54*(3), 592-614.

Nishizawa, C., Wang, J. Y., Sekine, S., & Saito, M. (2003). Effect of dietary DHA on DHA levels in retinal rod outer segments in young versus mature rats. *International Journal for Vitamin and Nutrition Research, 73*(4), 259-65.

Nomura, A., Shigemoto, R., Nakamura, Y., Okamoto, N., Mizuno, N., & Nakanishi, S. (1994). Developmentally regulated postsynaptic localization of a metabotropic glutamate receptor in rat rod bipolar cells. *Cell, 77*(3), 361-369. doi:10.1016/0092-8674(94)90151-1

Nussenblatt, R. B., & Ferris III, F. (2007). Age-related macular degeneration and the immune response: Implications for therapy. *American Journal of Ophthalmology, 144*(4), 618-626.e2. doi:10.1016/j.ajo.2007.06.025

Okano, K., Maeda, A., Chen, Y., Chauhan, V., Tang, J., Palczewska, G., et al. (2012). Retinal cone and rod photoreceptor cells exhibit differential susceptibility to light-induced damage. *Journal of Neurochemistry, 121*(1), 146-156. doi:10.1111/j.1471-4159.2012.07647.x

Querques, G., Forte, R., & Souied, E. H. (2011). Retina and omega-3. *Journal of Nutrition and Metabolism, 2011*, 12.

Ramkumar, H. L., Zhang, J., & Chan, C. (2010). Retinal ultrastructure of murine models of dry age-related macular degeneration (AMD). *Progress in Retinal and Eye Research, 29*(3), 169-190. doi:10.1016/j.preteyeres.2010.02.002

Raz-Prag, D., Ayyagari, R., Fariss, R. N., Mandal, M. N. A., Vasireddy, V., Majchrzak, S., et al. (2006). Haploinsufficiency is not the key mechanism of pathogenesis in a heterozygous Elovl4 knockout mouse model of STGD3 disease. *Investigative Ophthalmology & Visual Science, 47*(8), 3603-3611. doi:10.1167/iovs.05-1527

Ross, C. A., & Poirier, M. A. (2005). What is the role of protein aggregation in neurodegeneration? *Nature Reviews. Molecular Cell Biology, 6*(11), 891-898.

Rotenstreich, Y., Fishman, G. A., & Anderson, R. J. (2003). Visual acuity loss and clinical observations in a large series of patients with stargardt disease. *Ophthalmology, 110*(6), 1151-1158. doi:10.1016/S0161-6420(03)00333-6

Rotstein, N. P., Politi, L. E., German, O. L., & Girotti, R. (2003). Protective effect of docosahexaenoic acid on oxidative stress-induced apoptosis of retina photoreceptors. *Investigative Ophthalmology & Visual Science, 44*(5), 2252-2259. doi:10.1167/iovs.02-0901

SanGiovanni, J. P., & Chew, E. Y. (2005). *Progress in Retinal and Eye Research, 24*, 87.

SanGiovanni, J. P., & Chew, E. Y. (2005). The role of omega-3 long-chain polyunsaturated fatty acids in health and disease of the retina. *Progress in Retinal and Eye Research, 24*(1), 87-138. doi:10.1016/j.preteyeres.2004.06.002

Schnebelen, C., Pasquis, B., Salinas-Navarro, M., Joffre, C., Creuzot-Garcher, C., Vidal-Sanz, M., et al. (2009). A dietary combination of omega-3 and omega-6 polyunsaturated fatty acids is more efficient than single supplementations in the prevention of retinal damage induced by elevation of intraocular pressure in rats. *Graefe's Archive for Clinical and Experimental Ophthalmology, 247*(9), 1191-1203. doi:10.1007/s00417-009-1094-6

Sharma, R. K., O'Leary, T. E., Fields, C. M., & Johnson, D. A. (2003). Development of the outer retina in the mouse. *Developmental Brain Research, 145*(1), 93-105. doi:10.1016/S0165-3806(03)00217-7

Simon, E., Bardet, B., Grégoire, S., Acar, N., Bron, A. M., Creuzot-Garcher, C. P., et al. (2011). Decreasing dietary linoleic acid promotes long chain omega-3 fatty acid incorporation into rat retina and modifies gene expression. *Experimental Eye Research, 93*(5), 628-635. doi:10.1016/j.exer.2011.07.016

Smithers, L. G., Gibson, R. A., McPhee, A., & Makrides, M. (2008). Higher dose of docosahexaenoic acid in the neonatal period improves visual acuity of preterm infants: Results of a randomized controlled trial. *The American Journal of Clinical Nutrition, 88*(4), 1049-1056.

Soubias, O., Teague, W. E., & Gawrisch, K. (2006). Evidence for specificity in lipid-rhodopsin interactions. *Journal of Biological Chemistry, 281*(44), 33233-33241. doi:10.1074/jbc.M603059200

Soubrane, G., Haddad, W. M., & Coscas, G. (2002). Age-related macular degeneration]. *Presse Médicale, 31*(27), 1282-1287.

Streichert, L. C., Birnbach, C. D., & Reh, T. A. (1999). A diffusible factor from normal retinal cells promotes rod photoreceptor survival in an in vitro model of retinitis pigmentosa. *Journal of Neurobiology, 39*(4), 475-490.

doi:10.1002/(SICI)1097-4695(19990615)39:4<475::AID-NEU2>3.0.CO;2-#

Suh, M., Sauvé, Y., Merrells, K. J., Kang, J. X., & Ma, D. W. L. (2009). Supranormal electroretinogram in fat-1 mice with retinas enriched in docosahexaenoic acid and n-3 very long chain fatty acids (C24–C36). *Investigative Ophthalmology & Visual Science, 50*(9), 4394-4401. doi:10.1167/iovs.08-2565

Suh, M., Wierzbicki, A. A., & Clandinin, M. T. (1994). Dietary fat alters membrane composition in rod outer segments in normal and diabetic rats: Impact on content of very-long-chain (C ⩾ 24) polyenoic fatty acids. *Biochimica Et Biophysica Acta (BBA) - Lipids and Lipid Metabolism, 1214*(1), 54-62. doi:10.1016/0005-2760(94)90009-4

Swaroop, A., Chew, E. Y., Rickman, C. B., & Abecasis, G. R. (2009). Unraveling a multifactorial late-onset disease: From genetic susceptibility to disease mechanisms for age-related macular degeneration. *Annual Review of Genomics and Human Genetics, 10,* 19-43. doi: 10.1146/annurev.genom.9.081307.164350.

Tanito, M., Brush, R. S., Elliott, M. H., Wicker, L. D., Henry, K. R., & Anderson, R. E. (2009). High levels of retinal membrane docosahexaenoic acid increase susceptibility to stress-induced degeneration. *Journal of Lipid Research, 50*(5), 807-819. doi:10.1194/jlr.M800170-JLR200

Terre'Blanche, G., van, d. W., Bergh, J., & Mienie, L. (2011). Treatment of an adrenomyeloneuropathy patient with lorenzo's oil and supplementation with docosahexaenoic acid-A case report. *Lipids in Health and Disease, 10*(1), 152.

Thomas, J. L., Nelson, C. M., Luo, X., Hyde, D. R., & Thummel, R. (2012). Characterization of multiple light damage paradigms reveals regional differences in photoreceptor loss. *Experimental Eye Research, 97*(1), 105-116. doi:10.1016/j.exer.2012.02.004

Tian, N. (2004). Visual experience and maturation of retinal synaptic pathways. *Vision Research, 44*(28), 3307-3316. doi:10.1016/j.visres.2004.07.041

Vardi, N., & Morigiwa, K. (1997). ON cone bipolar cells in rat express the metabotropic receptor mGluR6. *Visual Neuroscience, 14*(4), 789-94.

Vasireddy, V., Jablonski, M. M., Mandal, M. N. A., Raz-Prag, D., Wang, X. F., Nizol, L., et al. (2006). Elovl4 5-bp–Deletion knock-in mice develop progressive photoreceptor degeneration. *Investigative Ophthalmology & Visual Science, 47*(10), 4558-4568. doi:10.1167/iovs.06-0353

Vasireddy, V., Uchida, Y., Salem, N., Kim, S. Y., Mandal, M. N. A., Reddy, G. B., et al. (2007). Loss of functional ELOVL4 depletes very long-chain fatty acids (≥C28 and the unique ω-O-acylceramides in skin leading to neonatal

death. *Human Molecular Genetics, 16*(5), 471-482. doi:10.1093/hmg/ddl480

Vasireddy, V., Wong, P., & Ayyagari, R. (2010). Genetics and molecular pathology of stargardt-like macular degeneration. *Progress in Retinal and Eye Research, 29*(3), 191-207. doi:10.1016/j.preteyeres.2010.01.001

Wang, S., Koster, K. M., He, Y., & Zhou, Q. (2012). miRNAs as potential therapeutic targets for age-related macular degeneration. *Future Medicinal Chemistry, 4*(3), 277-287. doi:10.4155/fmc.11.176

Wang, Z., Dillon, J., & Gaillard, E. R. (2006). Antioxidant properties of melanin in retinal pigment epithelial cells. *Photochemistry and Photobiology, 82*, 474–479.

Westheimer, G. (1984). Spatial vision. *Annual Review of Psychology, 35*(1), 201-226. doi:10.1146/annurev.ps.35.020184.001221

Williams, M. A., Craig, D., Passmore, P., & Silvestri, G. (2009). Retinal drusen: Harbingers of age, safe havens for trouble. *Age and Ageing, 38*(6), 648-654. doi:10.1093/ageing/afp136

Wisard, J., Faulkner, A., Chrenek, M. A., Waxweiler, T., Waxweiler, W., Donmoyer, C., et al. (2011). Exaggerated eye growth in IRBP-deficient mice in early development. *Investigative Ophthalmology & Visual Science, 52*(8), 5804-5811. doi:10.1167/iovs.10-7129

Yoshizawa, K., & Tsubura, A. (2005). Characteristics of N-methyl-N-nitrosourea-induced retinal degeneration in animals and application for the therapy of human retinitis pigmentosa. *Nihon Ganka Gakkai Zasshi, 109*(6), 327-37.

Zambiazi, R. C., Przybylski, R., Zambiazi, M. W., & Mendoca, C. B. (2007). Fatty acid compositions of vegetable oils and fats. *Curitiba, 25*(1), 111-120.

Zeiss, C. J. (2010). Animals as models of age-related macular degeneration. *Veterinary Pathology Online, 47*(3), 396-413. doi:10.1177/0300985809359598

Zhang HR. Scanning electron-microscopic study of corrosion casts on retinal and choroidal angioarchitecture in man and animals. *Progress in Retinal and Eye Research*. 1994;13:243–270.

Zhang, K., Kniazeva, M., Han, M., Li, W., Yu, Z., Yang, Z., et al. (2001). A 5-bp deletion in ELOVL4 is associated with two related forms of autosomal dominant macular dystrophy. *Nature Genetics, 27*(1), 89-93.

**Supplementary Material**

**A) Number of animals employed for each outcome measure**

**Table A: Number of animals employed for each outcome measure**

| | Outcome measures | | | |
|---|---|---|---|---|
| **Experimental Group** | **1 month ERG** | **3 month ERG** | **Anatomy** | **Lipid Profile** |
| WTChow | 10 | 10 | 4 | 3 |
| WT- | 9 | 8 | 6 | 5 |
| WT+ | 14 | 8 | 4 | 3 |
| TGChow | 12 | 11 | 7 | 6 |
| TG- | 11 | 10 | 5 | 9 |
| TG+ | 14 | 14 | 8 | 8 |
| **Total** | 70 | 61 | 34 | 34 |

Values for ERG measures represent number of animals, while values for "Anatomy" and "Lipid Profile" represent number of retinas

**B)**

**Table B. Fatty acid composition of vegetable oils used in custom diets.**

| | Olive Oil | Canola Oil | Coconut Oil | Corn Oil |
|---|---|---|---|---|
| ***Saturated Fatty Acids*** | | | | |
| Caprilic Acid, C8:0 | - | - | 6.4 | - |
| Capric Acid, C10:0 | - | - | 5.6 | - |
| Lauric Acid, C12:0 | - | - | 45.5 | - |
| Miristic Acid, C14:0 | - | 0.1 | 18.8 | - |
| Palmitic Acid, C16:0 | 10.8 | 3.8 | 10.1 | 10.5 |
| Margaric Acid, C17:0 | 0.1 | 0.0 | - | 0.1 |
| Stearic Acid, C18:0 | 3.6 | 1.9 | 4.3 | 2.0 |
| Arachidic Acid, C20:0 | 0.5 | 0.6 | 0.1 | 0.4 |
| Beheric Acid, C22:0 | 0.2 | 0.4 | - | 0.8 |
| Lignoceric Acid, C24:0 | 0.1 | 0.3 | - | 0.2 |
| *Total* | *15.3* | *7.0* | *90.7* | *13.9* |
| | | | | |
| ***Unsaturated Fatty Acids*** | | | | |
| Palmitoleic Acid, C16:1 | 0.9 | 0.2 | - | - |
| Miristoleic Acid, C17:1 | 0.2 | - | - | 0.1 |
| Oleic Acid, C18:1 | 75.6 | 62.4 | 7.5 | 24.2 |
| Linoleic Acid, C18:2 | 7.0 | 20.1 | 1.8 | 60.4 |
| α-Linolenic Acid, C18:3 | 0.7 | 8.4 | - | 1.0 |
| Gadoleic Acid, C20:1 | 0.3 | 1.5 | 0.1 | 0.3 |
| Eicosadienoic Acid, C20:2 | - | 0.1 | - | - |
| Erucic Acid, C22:1 | - | - | - | - |
| Docosadienoic Acid, C22:2 | 0.1 | - | - | - |
| Nervonic Acid, C24:1 | - | 0.3 | - | 0.2 |
| | | | | |
| ***Monosaturated Fatty Acids*** | 77.0 | 64.4 | 7.5 | 24.8 |
| | | | | |
| ***Polyunsaturated Fatty Acids*** | 7.7 | 28.6 | 1.8 | 61.4 |

Table adapted from results found in Zambiazi et al (2007). Numbers are expressed as w/w of total fatty acids.

**C) Full-field ERG: Square Flicker Response**

The flicker response test is performed under photopic conditions. In this protocol, animals are presented with bright flashes of light with increasing frequencies ranging from 3 to 60Hz within 13 steps. At higher frequencies, the recovery rate for phototransduction (or the visual cycle) in cone photoreceptors must occur faster in order to recognize the "flickering" of lights as individual flashes. If the frequency of the light presentation surpasses the phototransduction cascade recovery rate, the light is perceived as a continuous presentation. This is known as flicker fusion. A faster recovery rate is therefore indicated by a higher fusion point. Regarding data analysis, this point is reached when the peak amplitude (measured from the apex of the positive wave) falls below 10μV (Figure I).

**I**

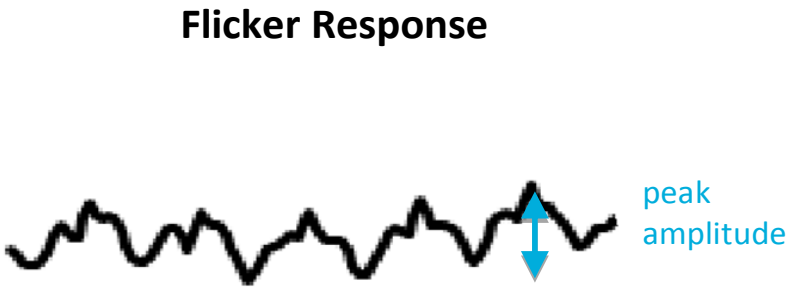


***Figure I.*** **Peak amplitude analysis for flicker response waves.** Peak amplitudes are measured to determine cone photoreceptor responsiveness to particular frequencies of slight stimulation.

### *C1) Flicker Response Results*

Genetic mutation and dietary manipulation had minimal effect on flicker responses at either 1 and 3 month time points (Figure II). Responses were inconsistent and sporadic; no significant differences amongst the groups were found. However, age had an effect on the mechanisms underlying the flicker response. Comparing the responses of 3 month (Figure IIC) animals to 1 month animals (Figure IIA), it was evident that there is was a reduction in peak amplitudes in older animals when looking at low frequency light stimulation. Moreover, flicker fusion frequencies occurred more quickly for 3 month compared to 1 month old mice. At 1 month most animals had a flicker fusion point of 55Hz (Figure IIB), but at 3 months the majority of animals fused at 50 Hz (Figure IID). As mentioned above, flicker fusion occurs when the recovery rate of the phototransduction cascade in photoreceptors is slower than the frequency of light being presented, making the stimulus appear seamless. An early fusion point, therefore, is an indication that regardless of genotype or diet, the efficiency of phototransduction declines as age increases. The effects of DHA, therefore, are not likely to be directly involved with the mechanisms of cone phototransduction.

**II**

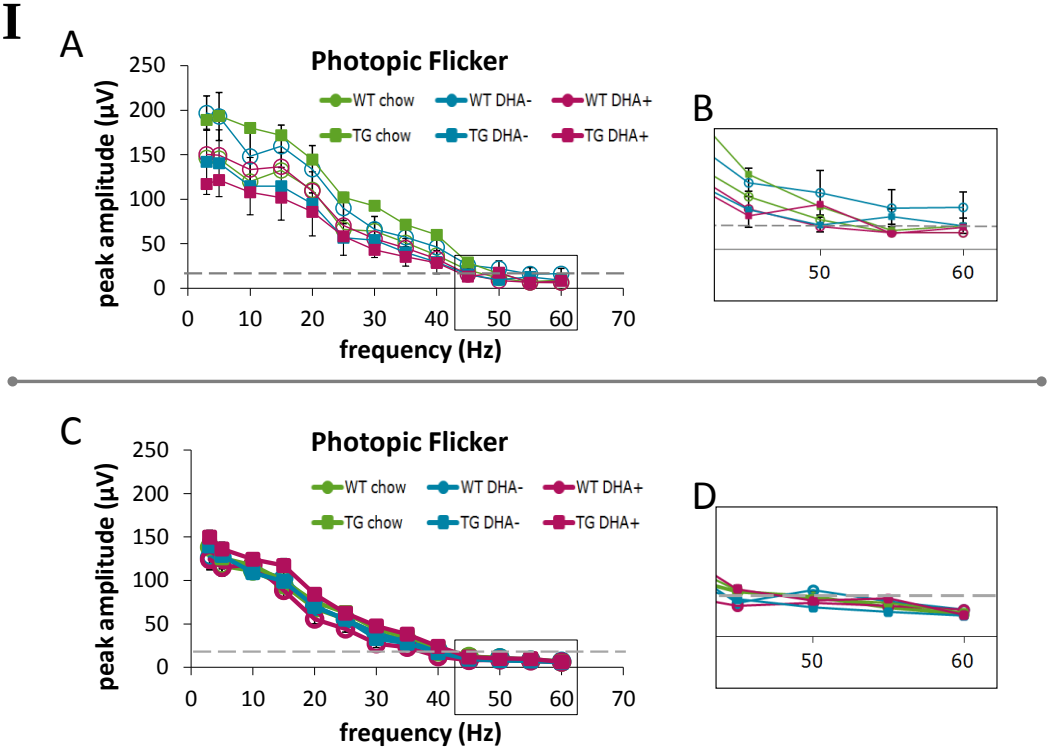


***Figure II.*** **Flicker responses at 1 and 3 months.** (A) Peak amplitude as a function of stimulus frequency at 1 month (B) Enlarged image depicting the 10 µV criterion between 45 and 60 Hz . (C) and (D) correspond to the images shown in (A) and (B) for data collected at 3 months. More variabilty exists at 1 month, but at 3 months all groups are behaving similarly. n=9-19.

**D) The effects of diet on photoreceptor numbers**

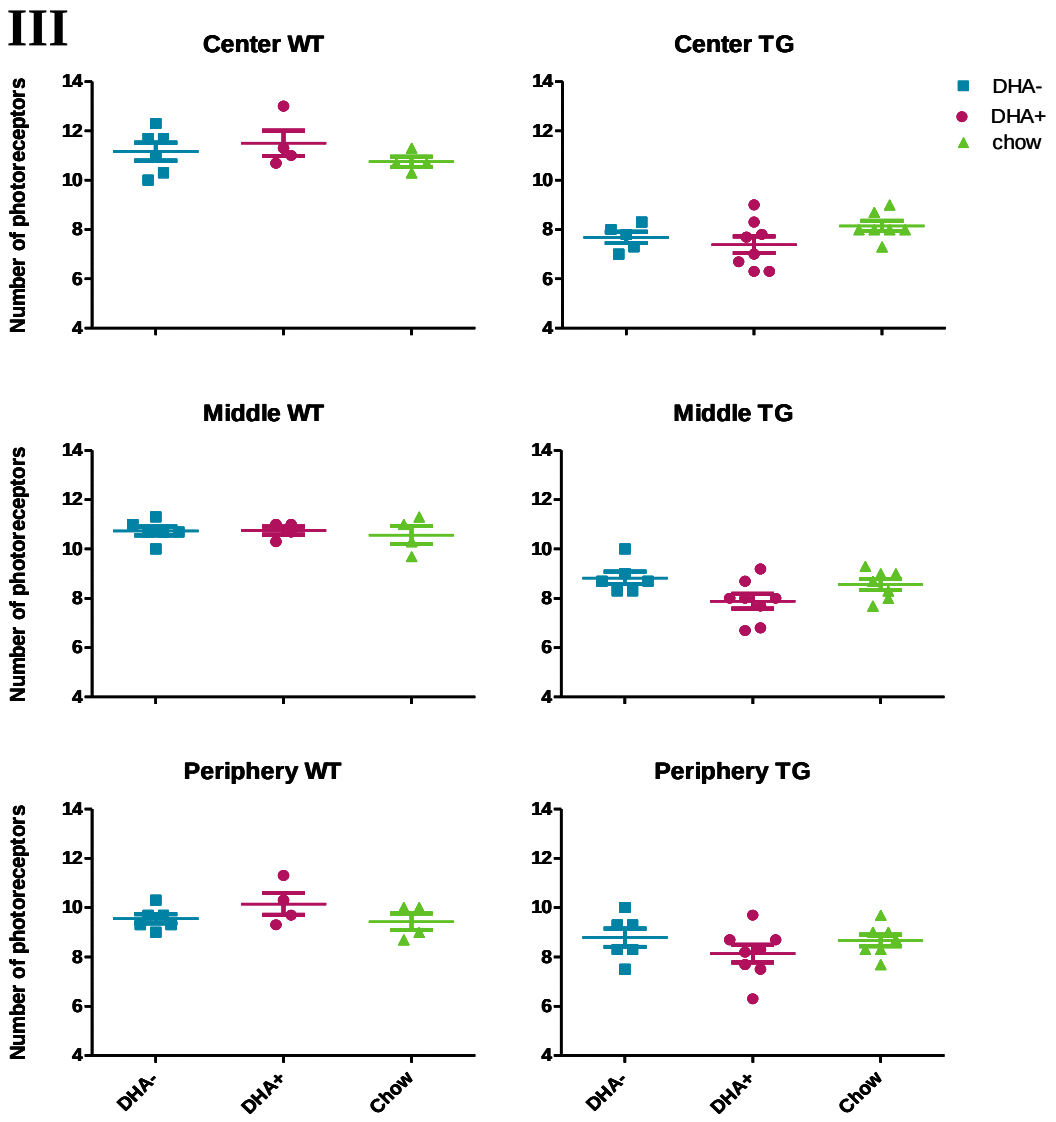


***Figure III.*** **The effects of diet on photoreceptor numbers.** No difference in the number of photoreceptors among diets. Variability, in TG animals compared to their WT counterparts is highlighted, especially in regards to the middle region of the retina. n=4-8.

**E) Chow fed retinal DHA and AA levels at 3 months**

Similar to findings described for TG DHA supplemented and non-supplemented animals, TG chow fed animals exhibited significantly lower retinal DHA and DHA/AA ratio levels (Figure IV, $p<0.05$). Again, AA levels were comparable between WT and TG retinas and more variablity was displayed in TG retinas. Overall, there was a 29% decrease TG retinas compared WT. Considering the high concentration of DHA typically found in rod outer segments (Nishizawa et al, 2003; Anderson et al, 2001), depletion of photoreceptors could contribute to the decline of retinal DHA levels in TG animals.

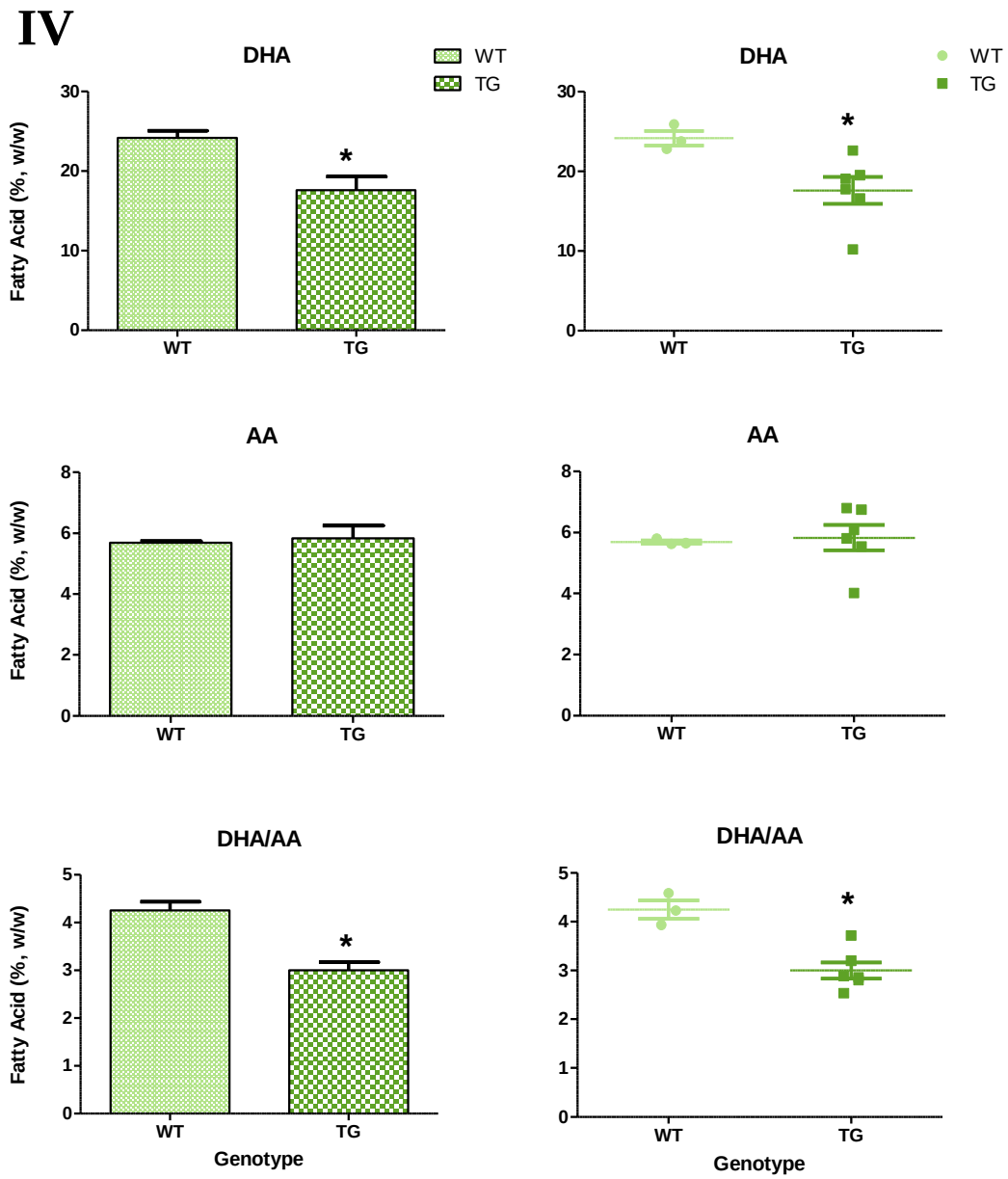


***Figure IV*. Chow fed retinal DHA and AA levels**. Significantly reduced DHA and DHA/AA levels in TG retinas. Variability in TG animals is emphasized in the right panel. n=3 and 6 for WT and TG, respectively. *p<0.05.

**F) Transgenic retinal omega 6 fatty acid levels at 3 months**

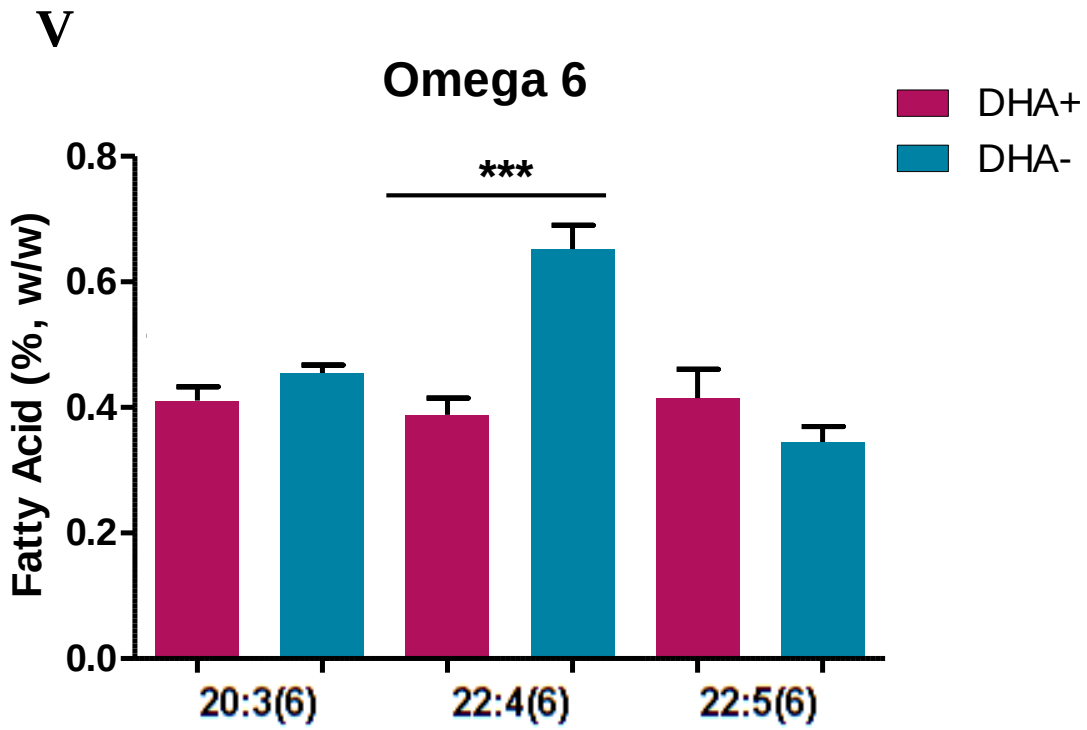


***Figure V.* Transgenic retinal omega 6 fatty acid levels**. DHA supplementation resulted in reduced 22:4(6) levels in TG retinas. ***P=0.0002. n=8 and 9 for TG+ and TG-, respectively. (Note: 20:4(6) - AA, was also found significantly lower in TG+ animals, but is not displayed).

**Table C. Transgenic retinal omega 6 fatty acid levels**

| | Omega 6 | | | | | | | |
|---|---|---|---|---|---|---|---|---|
| | 20:3(6) | | 20:4(6) ** | | 22:4(6) *** | | 22:5(6) | |
| | Mean | SE | Mean | SE | Mean | SE | Mean | SE |
| TG+ | 0.411 | 0.022 | *4.137* | *0.488* | *0.388* | *0.026* | 0.415 | 0.046 |
| TG- | 0.455 | 0.013 | *6.401* | *0.393* | *0.653* | *0.038* | 0.345 | 0.025 |

**G) Transgenic retinal omega 3 fatty acid levels at 3 months**

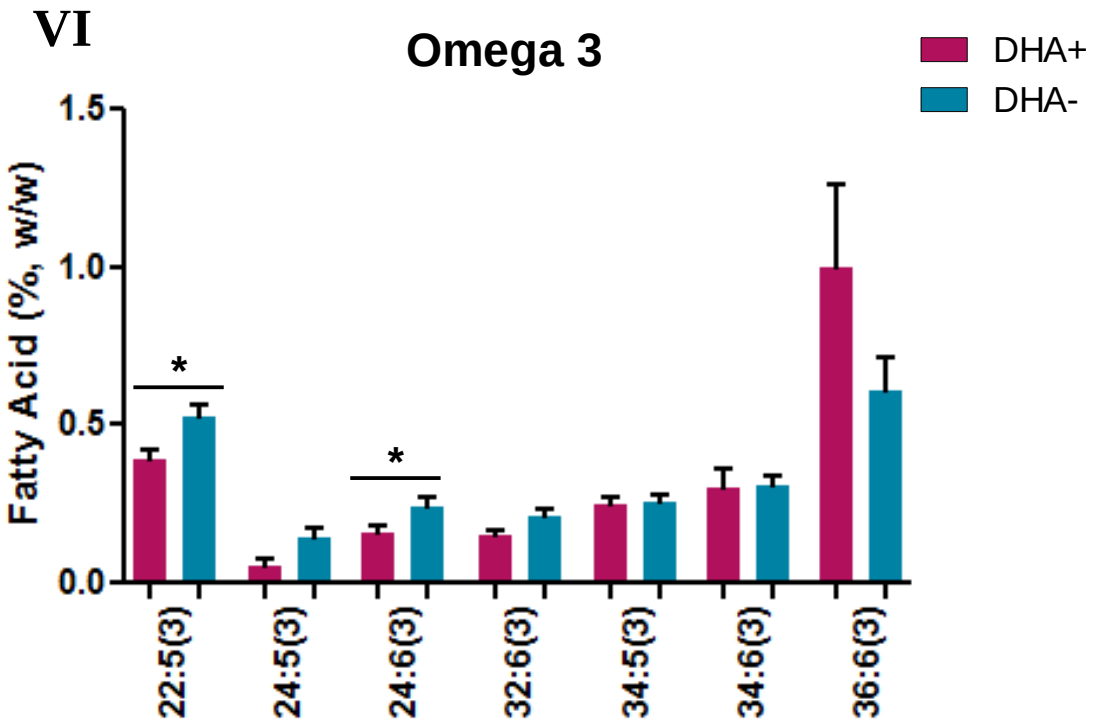


***Figure VI.*** **Transgenic retinal omega 3 fatty acid levels**. DHA supplementation resulted in decreased 22:5(3) and 24:6 (3) in TG retinas. *$p<0.05$. n=8 and 9 for TG+ and TG-, respectively. (Note: 22:6(3) - DHA, was also found significantly lower in TG+ animals, but is not displayed)

**Table D. Transgenic retinal omega 6 (C22-C24) fatty acid levels**

| | Omega 3 | | | | | | | |
|---|---|---|---|---|---|---|---|---|
| | 22:5:(3) * | | 22:6(3) * | | 24:5(3) | | 24:6(3) * | |
| | Mean | SE | Mean | SE | Mean | SE | Mean | SE |
| TG+ | *0.395* | *0.026* | *8.198* | *1.508* | 0.051 | 0.027 | *0.163* | *0.021* |
| TG- | *0.526* | *0.041* | *13.320* | *1.594* | 0.144 | 0.033 | *0.243* | *0.026* |

**Table E. Transgenic retinal omega 6 (C32-C36) fatty acid levels**

| | Omega 3 | | | | | | | |
|---|---|---|---|---|---|---|---|---|
| | 32:6(3) | | 34:5(3) | | 34:6(3) | | 36:6(3) | |
| | Mean | SE | Mean | SE | Mean | SE | Mean | SE |
| TG+ | 0.154 | 0.013 | 0.249 | 0.023 | 0.301 | 0.057 | 1.002 | 0.257 |
| TG- | 0.213 | 0.023 | 0.258 | 0.017 | 0.306 | 0.032 | 0.605 | 0.109 |

**H) Fatty acid metabolic pathway in transgenic animals**

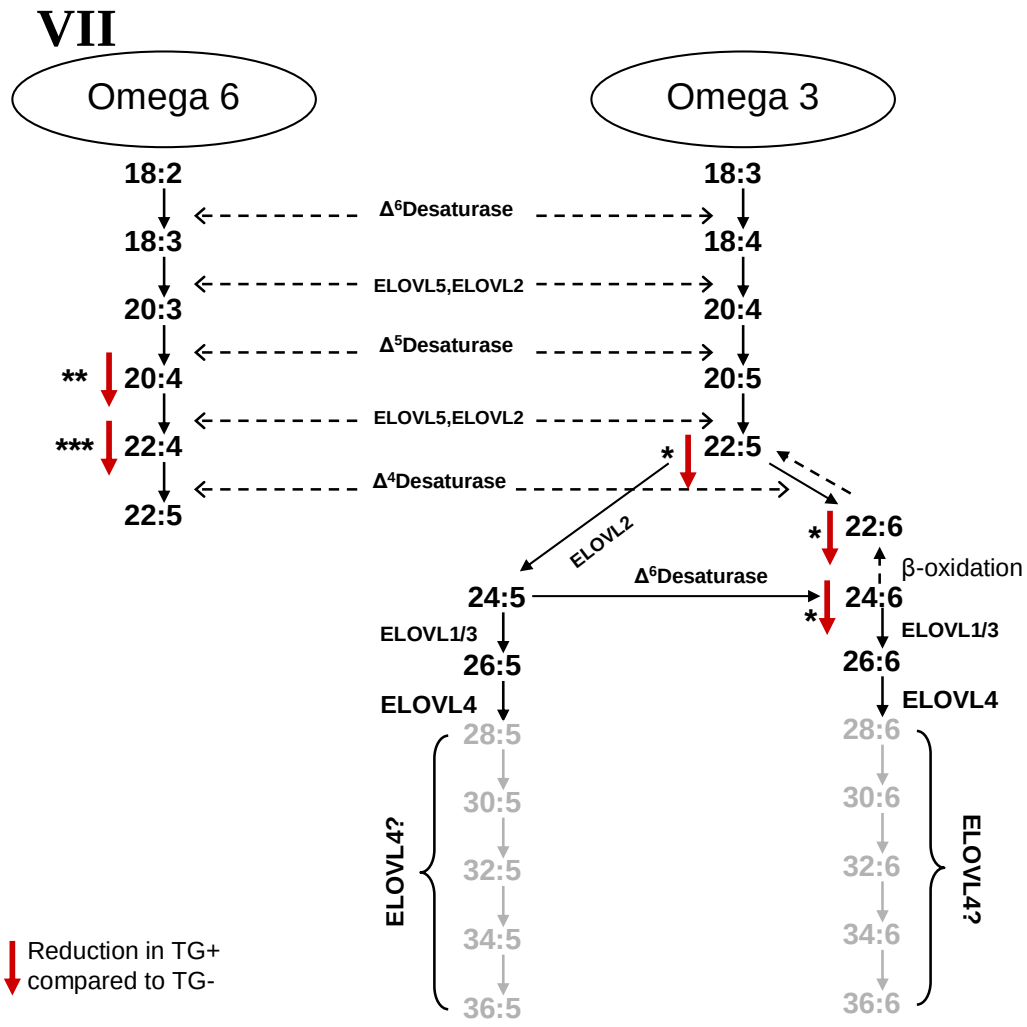


***Figure VII.*** **Fatty acid metabolic pathway in transgenic animals**. DHA supplementation decreases both omega-6 and 3 fatty acids, though it appears that it has a more significant effect on the omega 6 metabolic pathway. Omega-6 and 3 C18 FA were undetected as were omega 3 C26-C30 FA. *p<0.05, **p<0.005, and ***P<0.0005. n=8-9.

**I) Preliminary findings from fundoscopy**

# VIII

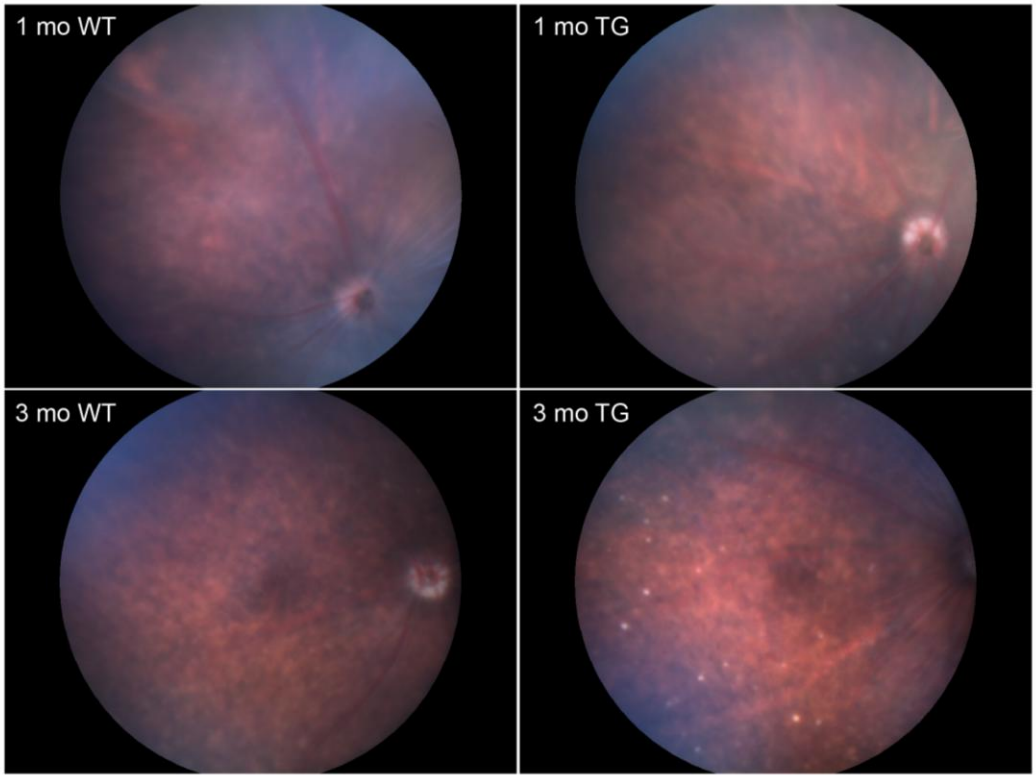


***Figure VIII.*** **Representative fundus photographs of chow fed mice.** At 1 month, no apparent differences in retinal health are observed between WT and TG mice. However, by 3 months extracellular deposits (white spotting) are detected in the temporal region of TG retinas. Images were obtained using a Micron III Retina Imaging System for rodents (Phoenix Research Laboratories, Inc, Pleasanton, CA) with whitelight brightfield imaging (Semrock FF01-554/211 filter; 450-680nm) and StreamPix5 software.